"Investigating the Immunoreactivity of Inhibitors of Axonal Regeneration in an Animal Model of Amyotrophic Lateral Sclerosis"

Eleni Voukali, BSc

Supervisor: Dr. Anthony Pullen

Institute of Neurology

Sobell Department of Motor Neuroscience

and Movement Disorder

Submitted as partial fulfilment of the requirements for the Msc in Clinical Neuroscience

University of London

July 2007

MSc Clinical Neuroscience
2006/07

ProQuest LLC
789 East Eisenhower Parkway
P.O. Box 1346
Ann Arbor, MI 48106-1346

ACKNOWLEDGEMENTS

I would like to acknowledge my supervisor Dr. Anthony Pullen firstly for being a model scientist and outstanding teacher and for carrying out the anaesthesia and perfusion fixation procedures outlined in the methodological part of this report. I must also mention my colleague Dimitra Athanasiou who conducted the genotyping and tissue preparation procedures and for providing me support, advice and encouragement throughout my thesis.

ABBREVIATIONS

ALS: Amyotrophic Lateral Sclerosis

BSA: Bovine Serum Albumin

CCS: Copper Chaperone for SOD1

CNS: Central Nervous System

DAB: Diaminobenzidine

ER: Endoplasmic Reticulum

GAP-43: Growth Associated Protein 43

NGS: Normal Goat Serum

Ods: Oligodendrtocytes

PBS: Phosphate Buffered Saline

PCR: Polymerase Chain Reaction

RTN: Reticulon Family

SOD1: Superoxide Dismutase 1

Tg: Transgenic

Wt: Wild Type

CONTENTS

ABSTRACT

Amyotrophic Lateral Sclerosis is a devastating neurodegenerative disease that affects motor neurons. Many theories about mechanisms contributing in its pathogenesis have been suggested. There is also evidence for alterations in synaptic plasticity during the progress of ALS. In particular, the expression of axonal growth promoting molecules like GAP-43, responsible for axonal regeneration, have been suggested to be sustained during the disease. On the other hand, axonal inhibitory molecules like Nogo-A seem to play an important part in compensating this regeneration attempt. In order to investigate the role of these two participating proteins during the preclinical and clinical stages of ALS, the spinal cord of SOD1 mice, the animal model mimicking one genetic form of ALS, have been examined. Using immunocytochemistry, immunoreactivity of Nogo-A and GAP-43 was shown in spinal cord sections of 6, 13 and 18 weeks of age. Our results suggest that Nogo-A has increased immunoreactivity in the oligodentrocytes in the ventral horns in grey matter of the spinal cord of the clinical Tg SOD1 mice and in the ventral white matter during preclinical and clinical stages. Increased immunoreatcivity was also found in the ventral horn neurons of the 13 weeks Tg mice compared to the other stages. GAP-43 has also shown greater immunoreactivity in Tg mice relating to the controls. These results suggest that a regeneration attempt is likely to happen during ALS but is maybe compensated by the inhibition of axonal growth at the later stages.

INTRODUCTION

Amyotrophic Lateral Sclerosis (ALS) is a late-onset progressive neurodegenerative disease that affects motor neurons (Delisle & Carpenter, 1984). The name is drawn from Jean-Martin Charcot, the biologist and clinician who first described it 136 years ago. He observed a distinct myelin pallor in the lateral portions of the spinal cord, representing degeneration and loss of the axons of upper motor neurons, as they descend from the brain to connect directly or indirectly onto the lower motor neurons within the spinal cord.

Approximately 5-10% of ALS cases are familial (inherited), which means that the majority of cases are sporadic or else, they do not have an obvious genetic component. The age of onset is between 45 and 60 and the typical disease course is up to 5 years. ALS affects 2-5:100,000 individuals in the population, with a 1:1,5 male:female ratio. In UK, the frequency of new cases per year is about 1,200-1,500.

The pathology of ALS involves selective dysfunction and death of the motor neurons with reactive gliosis. Sporadic and familial forms of ALS produce similar pathologic hallmarks. The most salient clinical features are spasticity, hyperreflexia (upper motor neurons), generalized weakness, muscle denervation, atrophy and paralysis (lower motor neurons). This

particularly, involves degeneration and loss of large pyramidal neurons in cortex, certain cranial motor nuclei and anterior horn cells in the spinal cord. In the end stage of the disease there is significant loss of large myelinated fibers in the corticospinal tracts and ventral roots as well as evidence of Wallerian degeneration and atrophy of the myelinated fibers (Picture 1. 1).

However, two groups of otherwise typical motor neurons are characteristically spared: firstly, the sacral motor nucleus of Onufrowitz (Onuf's nucleus), which innervates muscles of the pelvic floor and associated sphincters and correlates with retention of urinary and faecal continence throughout the illness and, secondly, motor neurons of third, fourth and sixth cranial nerves which innervate the external ocular muscles, so that retention of normal eye movements is a typical feature of the disease (Brown *et al.*, 2000). The basis of this selective sparing is likely to involve complex interactions of the physiological and biological properties of these neuronal groups (expression of cytoplasmic calcium buffering proteins, lack of direct monosynaptic corticospinal innervation, differences in glutamatergic neurotransmission and nitric oxide metabolism) which relate to some of the probable disease mechanisms further explained below.

Although ALS is a disease with its main thrust on the motor neurones, there is increasing evidence of a wider system involvement. Thus, sometimes degeneration also occurs in Clarke's column, spinocerebellar tracts, posterior columns and substantia nigra. Sensory axons may show spheroids in the

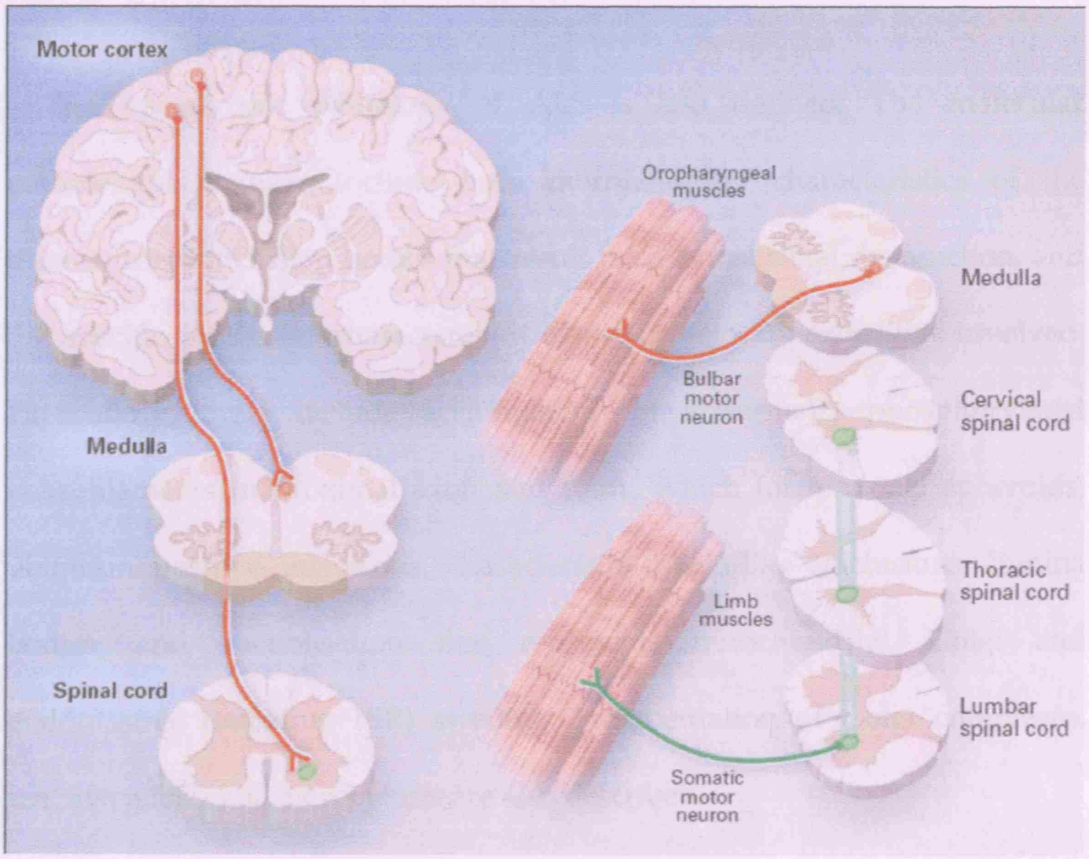

Picture 1. 1. Motor Neurons Selectively Affected in ALS (from Rowland & Schneider, 2001).

central nervous system (CNS) and abnormal sensory evoked potentials have additionally been described.

The microscopic pathology of ALS is less defined. The molecular pathological changes include both morphological characteristics of the intraneuronal inclusion bodies that result from cytoskeletal dysfunction, and the specific molecular characteristics of the protein abnormalities involved. Particularly, these include accumulation of abnormally phosphorylated neurofilaments in proximal axon and soma, which form axonal spheroids, ubiquitin positive inclusions, characteristic "skein-like" inclusions, Bunina bodies, and vacuolisation that represents mitochondrial, Golgi and endoplasmic reticulum (ER) swelling. Fragmentation of Golgi complexes, reactive gliosis and astrocytosis are also described.

Theories of ALS pathogenesis

Multiple theories have been proposed to explain the molecular pathogenesis of ALS. It is likely that more than one of these mechanisms contributes to human ALS, but it remains to be explained how these pathways interact. Thus, selective vulnerability of motor neurons likely arises from a combination of several mechanisms, including SOD1 gene defect, protein misfolding, mitochondrial malsfunction, oxidative damage,

excitotoxicity, glial associative toxic damage and neurotrophic abnormalities (Picture 1. 2).

Gene Defect - Mutation in Gene Encoding Superoxide Dismutase 1 (SOD1). Mutations in the SOD1 gene are the most common form of inherited ALS (Boillee *et al.*, 2006), underlying 20% of all familial ALS cases. Although overall only 2% of patients with ALS have a mutation in SOD1, the discovery of these mutations was a landmark in ALS research because it provided the first molecular insights into the pathogenesis of the disease. SOD1 is an enzyme that requires copper and catalyses the conversion of toxic superoxide radicals to hydrogen peroxide and oxygen. A copper atom at the active site mediates catalysis. SOD1 also has pro-oxidant activities, including peroxidation, the generation of hydroxyl radicals and the nitration of tyrosine. Since free copper is highly reactive and toxic, it must be loaded onto SOD1 by a copper chaperone for SOD1 (CCS) and subsequently held in place by a conserved disulfide bond whose formation is catalyzed by the CCS (Furikawa *et al.*, 2004). Inefficient incorporation of copper into SOD1 and/or a decreased shielding of copper (due to changes in SOD1 structure as a result of mutation) could provide an opportunity for aberrant copper-dependant oxidative chemistry, yielding cellular damage and motor neuron degeneration.

Oxidative Damage Giving rise to Apoptosis, Mitochondrial Dysfunction. Mutant SOD1 may catalyse aberrant biochemical reactions, resulting in the

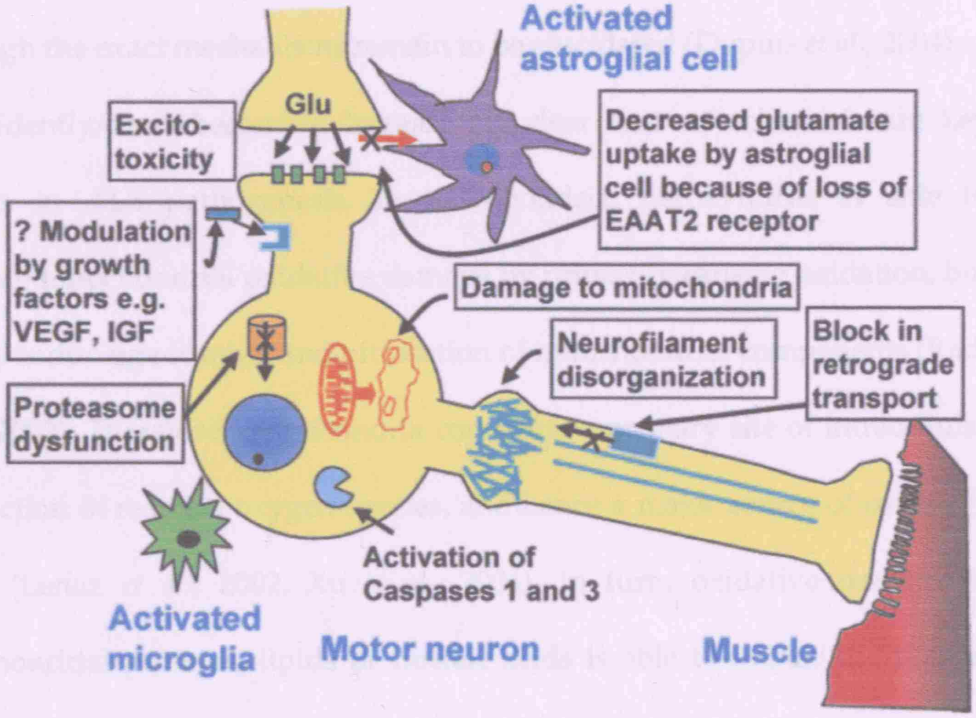

Picture 1. 2. Convergence of Multiple Pathways that May Damage Motor Neuron (Bruijn *et al.* 2004).

production of potentially damaging reactive oxygen species (ROS), such as the superoxide anion ($O_2^{\bullet -}$), the hydroxyl radical ($OH^{\bullet}$), hydrogen peroxide (H_2O_2), and peroxynitrite ($ONOO^-$) (Cluskey & Ramsden, 2001). Peroxynitrite formed in the cytoplasm might diffuse into the mitochondria, although the exact mechanisms remain to be elucidated (Dupuis *et al.*, 2004).

Evidently, it is becoming increasingly clear that mitochondria are key players in ALS pathogenesis. In mitochondria, peroxynitrite is able to promote mitochondrial oxidative damage by primarily causing oxidation, but also by inducing nitration and nitrosation of mitochondrial components (Radi *et al.*, 2002). Therefore, mitochondria constitute a primary site of intracellular production of reactive oxygen species, and hence a major source of oxidative stress (Lenaz *et al.*, 2002, Xu *et al.*, 2004). In turn, oxidative damage to mitochondrial proteins, lipids or nucleic acids is able to impair the normal function of mitochondria (Boillee *et al.*, 2006). There are histopathological observations of vacuolated and dilated mitochondria with disorganised cristae and membranes in the motor neurons (and muscle) of both sporadic and familial ALS patients (Afifi *et al.*, 1966, Hirano *et al.*, 1984a, b).

In ALS, motor neurons most likely die as a result of apoptosis. Mitochondria are the gatekeepers of apoptosis, with the opening of the permeability transition pore and release of cytochrome c central to the cascade of caspase proteases activation, in response to signals integrated by Bcl-2 proteins.

Excitotoxicity (Glutamate Transporter Abnormalities). Glutamate excitotoxicity might contribute to neurodegeneration in ALS (Rothstein *et al.*, 1990). Glutamate activity at the synaptic cleft is regulated by receptor inactivation and sodium/potassium coupled glutamate reuptake by transporter proteins (excitatory amino acid transporters; EAATs) in neurones and astrocytes. Oxidative damage to the EAAT2 glutamate transporter could feasibly lead to the accumulation of glutamate in the extracellular compartment and therefore to excitotoxic neuronal damage, thus linking oxidative damage with excitotoxicity (Cluskey & Ramsden, 2001).

Glial Associated Toxic Influence. The death of the motor neurons depends, at least in part, on a contribution from surrounding microglia and possibly other types of glial cells (Boillee *et al.*, 2006). Microglial cells, the macrophages of the CNS, have long suspected as central components in neurodegenerative diseases where their role may include secretion of trophic or toxic molecules. In ALS, microglial activation has been described in the brain and spinal cord of patients (Engelhardt & Appel, 1990, Henkel *et al.*, 2004, Kawamata *et al.*, 1992, McGeer *et al.*, 1991, Troost *et al.*, 1993, Turner *et al.*, 2004). The microglial reactivity is initiated before motor neuron loss (Henkel *et al.*, 2006).

Protein Misfolding is a probable initiating factor for formation of protein aggregates in ALS. Aggregate mediated inhibition of the proteasome machinery, decreased chaperone activity, deregulation of organelle function

including Golgi, ER and mitochondria, and axon transport defects are possibly linked to aberrant accumulations of intermediate filaments. The aggregates found in ALS patients contain ubiquitin, a protein adduct which typically targets proteins for disposal via the proteasome. Mis-accumulation of ubiquinated, misfolded proteins might adversely affect the proteasome machinery and impair normal protein degradation. The contribution of these protein aggregations to motor neuron toxicity remains to be established. (Boillee *et al.*, 2006). In particular, are accumulations toxic themselves or protective in that they remove potentially harmful substances from the system and package them into a neurotoxic structure?

Neurotrophic Abnormalities. Neurotrophic factors selectively regulate the growth and survival of certain populations of neurons in the central and peripheral nervous systems (Bruijn *et al.* 2004). They have an essential role in neuronal development and in the maintenance of differentiated neurons. Because astrocytes and microglia are important sources of neurotrophic factors, damage to those cells as occurs pathologically in ALS (Borchelt, 2006), suggests that loss of trophic support is one of the underlying factors causing motor neuron degeneration. The trophic factors that may be involved in ALS pathogenesis include brain-derived neurotrophic factor, glial cell line-neurotrophic factor (GDNF), insulin like growth factor (IGF-1) and abnormal functioning of vasoendothelial growth factor (VEGF).

Transgenic Mice

Recent success in using transgenic mouse technology to produce animal models of neurodegenerative diseases is rapidly advancing the understanding of pathogenic mechanisms and facilitating the search for effective therapeutics (Brown et al., 2000). The use of transgenic technology has allowed the creation of genetically exact (but with some phenotypic differences) models of the human disease. The type of transgenics may be:

- Overexpressors that express extra copies of gene
- Underexpressors that express one allele of a gene
- Knock out in which the gene is removed
- Mutants that express an altered gene

Since disease is initiated by a mutant human protein, such models open a window to the exploration and ultimately to the understanding of complex disease processes that in patients would otherwise remain closed. The short lifespan of the mouse allows for efficient investigation of age related neurodegenerative processes that require many years to develop in primates and humans. Thus, transgenics provide an accurate model of the disease to test therapeutic strategies and contribute to the understanding of the disease. The only difference is the extent to which the pathology resembles the human disease. A good animal model should resemble the disorder in aetiology, biochemistry, symptomology and treatment.

The identification of SOD1 as a causative gene in ALS allowed the generation of multiple lines of transgenic mice, which exhibit a transgene dose-dependent ALS-like pathology. Given the cytopathological and pathophysiological similarities between sporadic and familial forms of ALS, it is generally accepted that these transgenic mice are valuable animal models for the analysis of the pathogenic mechanisms leading to ALS. Thus, most of the knowledge obtained so far on mechanisms of motor neuron pathology in ALS is from studies using these models. In particular, transgenic mice expressing either G93A or G37R human SOD1 have elevated SOD1 activity levels and develop progressive hindlimb weakness and muscle wasting between 4 and 6 months of age (Wong *et al.*, 1995, Bruijn *et al.*, 1997). Additionally, low levels of accumulated human G85R SOD1 are sufficient to cause severe motor neuron disease without altering the protein and activity levels of endogenous SOD1. G86R also expresses a mutation of the murine SOD1 gene corresponding to human G85R (Ripps *et al.*, 1995). The A4V mutation of the SOD1 gene, responsible for 50% of human FALS, fails to induce disease in mice.

All SOD1 mutant mice have normal motor function for the first few months of life but then show accelerative weakness in hindlimbs. The age of onset varies with particular mutation and with transgene copy number. The higher the transgene copy number, the earlier the onset of symptoms is expressed. Weakness deteriorates rapidly, paralysis and death within 10-15

days of onset of symptoms in all transgene lines (Morrison *et al.*, 1998a). The clinical features involve loss of upper and lower motor neuron centres and therefore spasticity, clonus, hyperreflexia, crossed spread of spinal reflexes, tremor (in G37R and G93A) severe paralysis, muscle atrophy and loss of weight and respiratory insufficiency (Chiu *et al.*, 1995, Gurney, 1997).

A two step process occurs in which damage mediated by free radicals accumulates to a threshold that triggers catastrophic motor neurone loss. Hence, pathological damage accumulates gradually through neurofilament disruption and glutamate excitotoxicity (Chiu *et al.*, 1995, Morrison et al., 1998b), astrocytosis, activation of microglia (in the facial nucleus in G93A mice, Mariotti & Bentivoglio, 2000), ubiquitin complexes in pathological cytoplasmic filaments in motor neurons dendrites and glia, cytoskeletal abnormalities, Golgi complex fragmentation, cytoplasmic ubiquitination, axonal swellings through neurofilament accumulation, Lewy-like bodies (Stieber *et al.*, 2000a, b), vacuolation of axons preceding vacuolation of the cell body and both of these changes preceding cell death by apoptosis. Aggregates of mutant protein appear in dendrites, in periaxonal processes of oligodentrocytes and in neuronal and astrocytic perikarya of G93A mice (Steiber *et al.*, 2000c). Subsequently, the above data suggest that transgenic mice overexpressing mutant SOD1 provide an excellent in vivo animal model of human ALS (Elliott *et al.*, 1999).

Compensatory Axonal Outgrowth in ALS

However, there is evidence suggestive of synaptic reorganisation and temporary motoneuronal recovery in ALS. McComas (1991) implies that some surviving motor neurones enlarge their peripheral territories through axonal sprouting, being therefore sufficient to maintain the muscle compound action potentials and twitch tensions within normal limits. However, once the motor unit loss accelerates, collateral reinnervation is no longer able to provide full functional compensation. In addition, Osei-Lah *et al.* (2004) suggest an abnormality of cortical or spinal interneurones inhibition, which suppresses the fast-conducted activity, resulting in a synaptic reorganisation favouring the inputs of the indirect pathway. Other experiments (Geracitano *et al.*, 2003) indicate that the molecular machinery for Long Term Depression (LTD) expression is present in G93A+ mice, but is partially impaired and masked by a predominant, NMDA receptor-dependent, Long Term Potentiation (LTP). Finally, an analysis (Perrin *et al.*, 2005) of SOD1 motoneurones during disease progression (early symptomatic stage, 90 day old; end stage of disease, 120 day old) showed a modest de-regulation of only three genes associated with cell death pathways, but a considerable up-regulation of genes involved in cell growth and/or maintenance.

One of these genes up-regulated in the study of Perrin *et al.* (2005) was the gene encoding the Growth Associated Protein. As Ikemoto *et al.* (1999) specify, Growth Associated Protein (GAP-43), a calmodulin-binding

phosphoprotein located on the cytoplasmic side of the plasma membrane (Gorgels *et al.* 1989), is a major protein of axonal growth cones (Benowitz & Routtenberg, 1987, Skene & Virag, 1989), the structures that are elaborated at the tip of growing axons specifically to inform function of motility and path finding, during axogenesis and regeneration. Accordingly, this protein is synthesised in the neuronal cell bodies, subsequently transported by fast axonal flow (Skene & Willard, 1981a, Skene & Willard, 1981b) and has been implicated in axonal growth and regeneration (Meiri et al., 1986).

Other recent evidence postulates that the GAP-43 is involved in the pathology of amyotrophic lateral sclerosis. Parhad *et al.* (1992) found increase in GAP-43 mRNA and the results of the study of Kage *et al.* (1998) suggest that the abnormal expression of GAP-43 mRNA, underlying the pathogenesis of ALS, is due to its quantitative increase and not due to qualitative abnormalities associated with a change in the amino acid sequences. In agreement with the latter, Ikemoto *et al.* (1999) provide information concerning plastic alterations of axonal terminals and synaptic remodelling in relation to motor neurone degeneration. They undertook an immunohistochemical study of GAP-43 expression in the anterior horns of ALS patients and they found that the most striking feature of GAP 43 expression in ALS was an increasing number of Anterior Horn Cells with dense accumulation of GAP-43 immunoreactivity on the surface of the cell bodies and proximal processes.

While the above evidence implies a capacity for synaptic re-organisation and axonal spouting in ALS, as a compensatory mechanism to maintain communication between different groups of neurones in the motor pathway and between motor neurones and muscle, this axonal outgrowth attempt may be constrained by the up-regulation of specific neurite outgrowth inhibitors, chiefly Nogo.

Nogo, a myelin associated protein (Brittis & Flanagan, 2001), has been reported to have three major transcripts, Nogo A, B and C (Chen *et al.*, 2000; GrandPre *et al.*, 2000; Prinjha *et al.*, 2000). Nogo belongs to the reticulon gene family (RTN) (Oertle & Schwab, 2003, Oertle *et al.*, 2003a), which consists of proteins 200-1200 amino acids in length, sharing a common C-terminus domain (reticulon homology domain). This domain is made of two hydrophobic regions along a 66 amino acid loop (Picture 1. 3). In the Nogo protein, this loop (Nogo 66) has captured intense interest, since it acts as potent inhibitor of neurite outgrowth, through its interaction with the NgR1 receptor complex (Schwab *et al.*, 2006, Oertle *et al.*, 2003b). The Nogo receptor complex comprises three proteins: the p75 co-receptor, which is probably the signally part of the complex (Wang *et al.*, *2002*), the transmembrane brain specific leucine-rich-repeat protein LINGO1 and the TROY (or TAJ). Besides Nogo A, other myelin growth inhibitory molecules bind to NgR1 as well, the myelin-associated-protein (MAG) and oligodentrocyte-myelin-glycoprotein (OMgp) (Fournier *et al.*, 2001). Hence, a sequence of secondary messenger mechanisms (involving α and γ secretases, EGF receptor) are integrated via

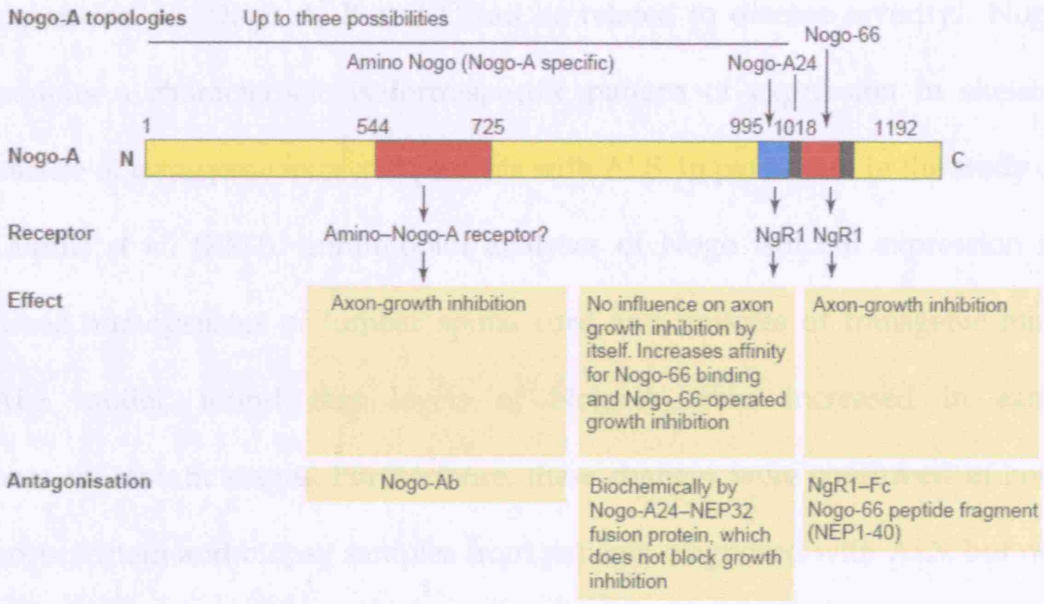

Picture 1. 3. The origin of myelin inhibition is based on the discovery of the axon-growth inhibitor Nogo-A. Nogo-A contains two inhibitory domains (red): Nogo-A544–725, which is located in the N-terminal part, and Nogo-66, which is located in the C-terminal part. Whereas the receptor of Nogo-66 (NgR1) has been identified, the receptor that binds to Nogo-A544–725 is still unknown. Up until now, three membrane topologies of Nogo-A have been proposed. (Taken from Schwab *et al.*, 2006)

the inhibitory myelin derived signal (Grandpre & Strittmatter, 2001, Teng *et al.*, 2004, 2006), that converges finally into intra-axoplasmic Rho activation and then to neurite growth inhibition (Picture 1. 4).

In view of that, the relevance of Nogo proteins as potential biomarkers of ALS has been documented, suggesting that alterations in the relative expression of Nogo A, B and C can be related to disease severity. Nogo exhibits a characteristic isoform-specific pattern of expression in skeletal muscle of transgenic mice and patients with ALS. In particular, in the study of Dupuis *et al.* (2002), immunoblot analyses of Nogo isoform expression in tissue homogenates of lumbar spinal cord and muscles of transgenic mice ALS model, found that levels of Nogo-A were increased in early presymptomatic stages. Furthermore, these changes were confirmed in both post-mortem and biopsy samples from patients diagnosed with ALS, but not control patients. Similar results were also obtained in the study of Jokic *et al.* (2005).

Collectively, the observations discussed above suggest that GAP-43 and Nogo-A are increasingly expressed during ALS progression. In the present study, the SOD1 mouse model of ALS will be used to a) investigate the distribution of Nogo-A and GAP-43 in the spinal cord of SOD1 mice and b) determine the first occurrence and the time course of Nogo and GAP-43 during pre-clinical and clinical phase of the ALS progression.

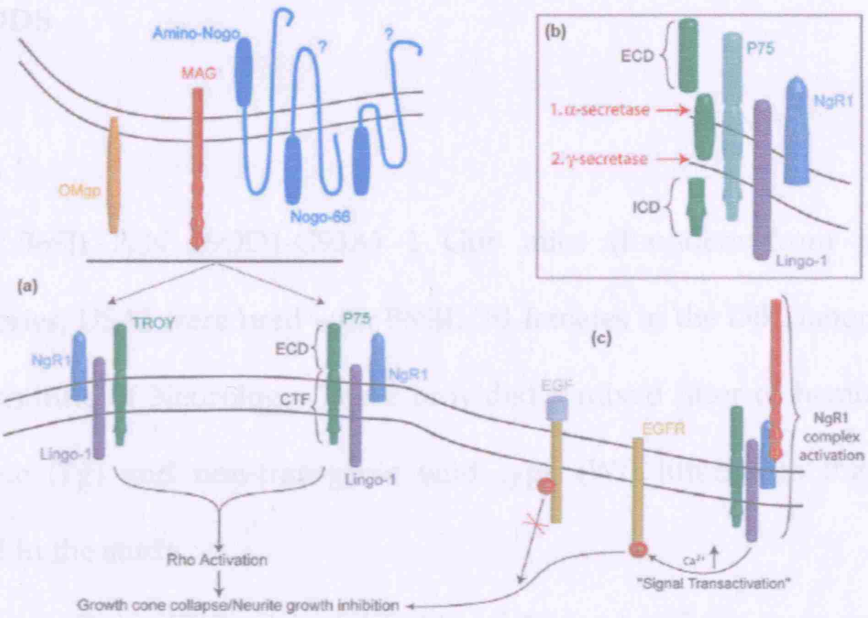

Picture 1 . 3. Involvement of the recently identified molecules Amino-Nogo-A, LINGO-1, TROY/TAJ, a-secretase and g-secretase, p75NTR shedding and EGF receptor in NgR1 signalling. (a) The inhibitory myelin ligands Nogo-A,MAG and OMgp bind to NgR1. NgR forms a trimeric complex with its co-receptors LINGO-1 and p75NTR. Activation of the NgR complex triggers a rapid rise of intracellular Ca2C, which results in the activation of the converging Rho pathway, leading to axonal-growth arrest and growth-cone collapse. In the absence of p75NTR, TROY acts as a functional homologue. (b) When p75NTR is part of the NgR complex, its sequential cleavage by a-secretase and g-secretase gives rise to an intracellular domain (ICD), which induces Rho activation. The a-secretase cleaves the extracellular domain (ECD) of p75NTR. The remaining membrane-bound C-terminal fragment of p75NTR (CTF) is further cleaved by intramembrane proteolysis (RIP) through g-secretase, resulting in the cytoplasmic release of ICD, which transmits the inhibitory signal. (c) A link of how the rise in intracellular Ca2C induces activation of Rho is provided by the EGF receptor (EGFR). Ca2C rise that is triggered by the NgR1complex leads to EGF-receptor phosphorylation, which, in turn, induces Rho activation. However, binding of EGF receptor to its ligand EGF does not induce Rho activation. This phenomenon of inter-receptor crosstalk is also referred to as trans-activation and is operated by the intracellular Ca2C rise (Taken from Schwab *et al.*, 2006).

METHODS

Animals

Male B6SJL-TgN (SOD1-G93A) 1 Gur mice (founders from Jackson Laboratories, USA) were bred with B6SJL/F1 females in the DBL laboratories of the Institute of Neurology. These provided a mixed litter of hemizygous transgenic (Tg) and non-transgenic wild type (Wt) littermates that were included in the study.

Five pairs of Tg and Wt mice of 4-6, 13 and 18 weeks of age were used. Wt littermates had normal mobility throughout a period extending to 200 days of age and hence were served as non-transgenic controls. Six and 13 weeks old Tg mice showed no muscle weakness and were therefore classified asymptomatic and formed the pre-clinical stage sample. Affected Tg mice of 18 weeks were classified symptomatic and formed the clinical stage sample. Onset of hind limb weakness with impaired movement in Tg males occurred at about 110 days and one or two days later in Tg females. Survival was defined by a veterinary approved end-point characterized by bilateral hind limb paralysis, loss of righting reflexes, body weight loss >15% over 3 days. Mean survival in males was 127.5 days and 130.6 days in females. All procedures described here were authorized by Home Office Approval, under personal and project Licences held by Dr Anthony Pullen.

Genotyping

Genomic DNA was isolated from tail biopsies comprising 0.5 cm lengths taken from the tip of tails of mice, using a kit and protocol distributed by Promega Inc. Each tail biopsy was put in a fresh, autoclaved 1.5 ml Eppendorf centrifuge tube and then digestion medium containing 120 µl of 0.5M EDTA (pH 8.0) and 500µl Nuclear Lysis Solution (Promega Cat No A7941) and 17.5µl of a 20mg/ml Proteinase K was added to each tube. After vortexing for 10-20 secs, the tubes were placed in a plastic rack in a water bath preheated to 55°C and incubated overnight at 55°C with occasional careful shaking to ensure the tissue is completely digested.

The next day, the tubes were removed from the water bath and after coming to room temperature, 200 µl protein precipitation solution (Promega A7951, 25ml) was added to each. Tubes were vortexed vigorously at high speed for about 20 secs and chilled on ice for 5 minutes. On seeing white protein precipitates, the tubes were transferred to a refrigerated centrifuge (Eppendorf Model 5402) and centrifuged for 6 minutes at 14,000g at 4°C. When a white pellet was formed the tubes were transferred to the rack and carefully un-caped in turn and the supernatant removed with a 200 µl micropipette fitted with a filtered 200 µl tip. The supernatants were transferred into clean autoclaved 1.5 ml Eppendorf centrifuge tubes and to each 600 µl isopropanol maintainned at room temperature was added in the volume ratio of 0.7 to 1X ; (~600µl to 750 µl supernatant) and carefully mixed

by inversion until the white thread-like strands of DNA were seen. The tubes were then were centrifuged for 1 min at 14,000g at room temperature to form a small white pellet of DNA, and the supernatant was pipetted out. Next, 600 µl 70% ethanol was added to each tube. Tubes were gently inverted several times to wash the DNA and centrifuged again at 14,000 g as above. The ethanol was aspirated and the tubes were re-centrifuged as above to remove all EtOH. After, the tubes were un-capped to air dry the pellet for 15 min before adding 200 µl autoclaved deionised water to each tube to re-hydrate the DNA. Finally the samples were left at room temperature for 1 hour and then were put in the fridge overnight ready for polymerase chain reaction (PCR) amplification.

On the third day, the pure DNA sample was amplified by the polymerase chain reaction (PCR) using primers IMR113, IMR114 to exon 4 of human G93A mutant SOD1. Primers for murine IL-2 (IMR042 and IMR043) were used for method control. PCR products were separated by electrophoresis on a 2% agarose gel containing ethidium bromide, and viewed by U-V trans-illumination. Tg mice with the mutant SOD1 gene expressed bands at ~236bp and their non-transgenic Wt littermates single bands at ~320bp.

Tissue Preparation and Freezing

Animals evaluated for immunocytochemistry were anaesthetised by intraperitoneal injection of a mixture of Domitor (Pfizer, UK, 1 mg/ml medetomidine HCL, 100mg/kg) and Ketaset (Fort Lodge, Uk, 100 mg/ml

ketamine HCI, 0.6 mg/kg), and perfused through the heart with firstly 50 ml of 20mM phosphate buffered saline (PBS) (pH 7.3) followed by 50ml 20mM PBS-buffered 4% paraformaldehyde-0.2% glutaraldehyde (pH 7.4) and finally 50 ml of the same fixative but now containing 10% sucrose. The spinal cords were removed, cut transversely into 3mm slices, post fixed for 24 hours in fixative containing 20% sucrose and transferred to PBS-30% sucrose solution for 24-36 hours before freezing.

Then the tissues were mounted on small pieces of cork (2x1cm x 2mm thick) placed inside aluminium foil cups of similar size (2x1x1cm). Orange-cap needles were inserted into the cork to support the tissue. The mounted tissue was frozen briefly in isopentane contained in a 100 ml beaker and cooled in liquid nitrogen, then covered 30% gum Arabic mountant and re-frozen in cooled isopentane. Next, the tissue was labelled, wrapped in silver foil and kept in -30°C until use (up to a maximum of 2-3 weeks).

Immunocytochemistry

Frozen tissue blocks were mounted on pre-cooled cryostat "chucks" with 30% gum Arabic. Serial sections (15μm in thickness) were cut perpendicular to the spinal cord axis on the cryostat at -22°C. After that, they were picked up on glass slides that had been previously coated with gelatine-chrome-alum solution (subbed) and air dried for 45-60 min.

Immunostaining was performed over 3 days using the strepavidin-biotin-peroxidase (SABC) method. On the first day, the sections were blocked with

5% Bovine Serum Albumin (BSA)- 5% normal goat serum (NGS) diluted in 20mM PBS-20mM glycine for an hour at room temperature, washed 3 times , 5 minutes each wash, with 20mM PBS-glycine containing 0.1% BSA, 0.1% NGS and incubated in primary antibody overnight at 4°C. Primary antibodies used were mouse monoclonal Anti-GAP-43 antibody from Sigma (cat No. G9264) and mouse anti-NOGO-A antibody from GSK (clone 6D5, Dupuis et al., 2002). Antibodies were diluted 1:2,000 and 1:1,000 respectively in 20mM PBS-glycine containing 1% BSA and 1%NGS.

On the second day, the slides were washed as described above prior to incubating in link antibody (biotinylated anti-mouse IgG diluted 1:200 in 20mM PBS-glycine containing 1% BSA and 1% NGS) for 4 hours at room temperature. Then the sections were washed as before, flooded with secondary antibody (biotinylated streptavidin horseradish peroxidase diluted 1:200 in 20mM PBS-glycine-0.1% BSA-0.1% NGS) and incubated overnight at 4°C.

On the third day, the sections were washed 3 times as described above with a fourth washing with 20mM PBS. Horseradish peroxidase streptavidin binding was visualised with diaminobenzidine (DAB) reagent (1.3mM diaminobenzidine-0.2% hydrogen peroxide made up in 5mM PBS). A constant development time of 3 minutes was used for each experiment. Finally, after had been washed 3 times (5 minutes per wash) with 20mM PBS, the slides were mounted in aqueous mountant 'Aquatex' (Agar).

For negative controls, the primary antibodies and link antibodies were omitted in separate tests.

Examination of Spinal Cord Sections

After staining, the slides were kept up to 3 days to allow mountant to fully penetrate tissue and dry. They were then examined on a Zeiss microscope connected to a 3.3Mpixel digital camera (Nikon, model Coolpix 995). For Nogo-A, sections of spinal cord were randomly selected for each sample at thoracic, lumbar, lumbosacral levels and examined in a prescribed sequence, covering in turn the ventral horns of grey matter and the dorsal and ventral regions of white matter. Three sets of photographs were taken for each experiment (1 per section). Microscope magnification (objective ×40), illumination temperature (5v, blue filter), sub-stage condenser aperture diameter, and camera 'zoom' magnification (3mm), were kept contact in each immunocytochemical experiment (Table 3. 1). Each photographic set consisted of four photographs depicting the:

1) right ventral horn
2) left ventral horn.
3) Dorsal white matter
4) Ventral white matter

A similar procedure for examination was undertaken for sections immunostained for GAP-43.

Qualitative and Quantitative analysis

Qualitative analyses of the immunoreactivity were undertaken in each the sections of spinal cord stained for Nogo A and Gap-43.

To further validate the qualitative results for Nogo-A, a quantitative analysis was conducted. Specifically, cellular staining densities and the numbers of stained cells per 1000μm^2 were analysed using Photoshop (Adobe Inc) and SigmaScan (JASC) image analysis software. The staining intensity was measured with a semi-quantitative method using the densitometer facility of Photoshop v 5.0 software. Mathematically, Optical density is = log10(1/T) where T is transmission which is a measure of the proportion of incident light passing through a specimen. Photoshop measures transmission, on a scale where 100% is equivalent to 100% transmission ('white') and 0% to 0% transmission ('black'). This can be used to measure the level of staining at a point on a feature (cell or background staining). The digital coloured photographs of the immunostained sections were convertedto grey-scale images, and 3 points on a feature were randomly selected with the indicator (mouse pointer) and their 'densities' recorded as three values on a 0-100% scale, and the mean of these three values was calculated. Thus, in each photograph, firstly the mean density value of the background staining (grey or white matter) was measured, and secondly, that of the stained neurones or oligodendrocytes.

The mean density value was calculated for each cell and finally, this mean value was then subtracted from the mean value for the background to take into account any variation in background between sections and experiments.

SigmaScan imaging software was used for measuring the average numbers of stained cells per 1000mm^2. First a calibration grid of 1000μm length was photographed five times at the same magnification, illumination, and camera settings as used to photograph sections. Each photo was called up in turn on SigmaScan and reduced to ×0.25 size. In this way, the numbers of pixels per 1000μm were measured for each calibration photographs, and the average value calculated. This gave a value of 51.70 pixels equal to 1 square micron.

Next, each photograph of an immunostained section was called up in SigmaScan, reduced in ×0.25 size, and the area (expressed as the total numbers of pixels) was measured for each. The area expressed in square microns was calculated and in conjunction with the numbers of stained cells in the region, the cell frequency was calculated and expressed as the average number of stained cells/1000mm^2. Analysis of cell frequency was conducted only for oligodendrocytes because of their particular relevance to Nogo-associated inhibition of axonal outgrowth. Ideally, the same procedure should be followed for neurones after calculating the different diameters and classifying neurones by size into putative motor neurones and interneurones. Unfortunately, this further analysis had to be omitted because of its time consuming nature and the time constraints of a 20 weeks project.

The data obtained were further statistically analysed using Excel (Microsoft Office) software. The t-test used was the Two sample assuming equal variancies to compare statistically the differences in the groups of the interest.

Counting criteria comprised cells that had staining observed in the cell body with the nucleus being devoid of staining (Buss et al. 2005). All stained neurones in ventral horn were counted because neurones in this area are mostly associated directly, or indirectly, with the motor function.

Photographs of spinal cord sections immunostained for Gap-43 were not analysed quantitatively because the pattern of immunoreactivity was diffused and scattered and not as discrete as for Nogo-A.

RESULTS

The immunoreactivity of Nogo-A and GAP-43 proteins were analysed using immunocytochemistry on sections of spinal cords from Tg and Wt mice. After genotyping to identify Tg and Wt mice, the mice were deeply anesthetized by intraperitoneal injection and perfused transcardially with fixative. Their spinal cords were removed, post-fixed and frozen. Cryostat sections of spinal cord were immunostained using the streptavidin-biotin-peroxidase method, and immunostaining was visualised with diaminobenzidine (DAB). The sections were then observed in the microscope, which was connected to a digital camera and photographs of ventral horn grey matter, and ventral and dorsal white matter were taken. The photographs were further analysed qualitatively for Nogo-A and Gap-43 and quantitatively for Nogo-A.

Genotyping

The classification of the animals derived from genotyping is stated in Table 3.1. Tg mice of 6 and 13 weeks of age that showed no muscle weakness, were classified as asymptomatic and formed the pre-clinical stage sample. Mice of 18 weeks, that showed muscle weakness, formed the clinical stage sample.

	6 weeks	13 weeks	18 weeks
Wt	Q#9	C#6	AD#2
	R#6	D#5	G#1
	R#11	E#5	G#2
	S#7	K#1	G#3
		E#3	G#4
Tg	Q#8	D#4	H#2
	Q#10	G#5	B#1
	R#7	I#2	C#1
	R#8	F#3	E#4
		O#8	JAX#A2

Table 3. 1. Classification of Animals According to the Results of Genotyping Experiments.

Qualitative Analysis of Nogo-A and GAP-43 Immunoreactivity.

An overview of the distribution of Nogo-A and Gap-43 can be seen in Plates 3. 1-6. A more detailed description is presented below.

Nogo-A

Nogo-A staining was detected in neurones in the ventral horn grey matter and in the oligodendrocytes (Ods) of the ventral horns in grey matter and of the ventral and dorsal white matter. The pattern of staining was differently distributed between the cells. Thus, there were cells that were positively stained and others that were negatively stained. In between, there was a mixture of heavier and lower staining. The different segmental levels of spinal cord, cervical, thoracic, lumber and sacral did not seem to be stained differently.

Wild type animals showed similar pattern of staining at all stages, clinical and pre-clinical. Hence, there was an equivalent amount of immunoreactivity in the ventral horn grey matter for Ods at the stage of 18 weeks, 13 weeks and 6 weeks. In the white matter there was a trend towards increased staining of Ods in the dorsal white matter. In the ventral white matter there was a moderate level of staining at all stages.

Tg animals of 18 weeks showed increase in the number of stained Ods in the ventral horn grey matter (Plate 3. 2). The Tg preclinical mice of 13 weeks and 6 weeks showed similar staining to the corresponding Wt sample.

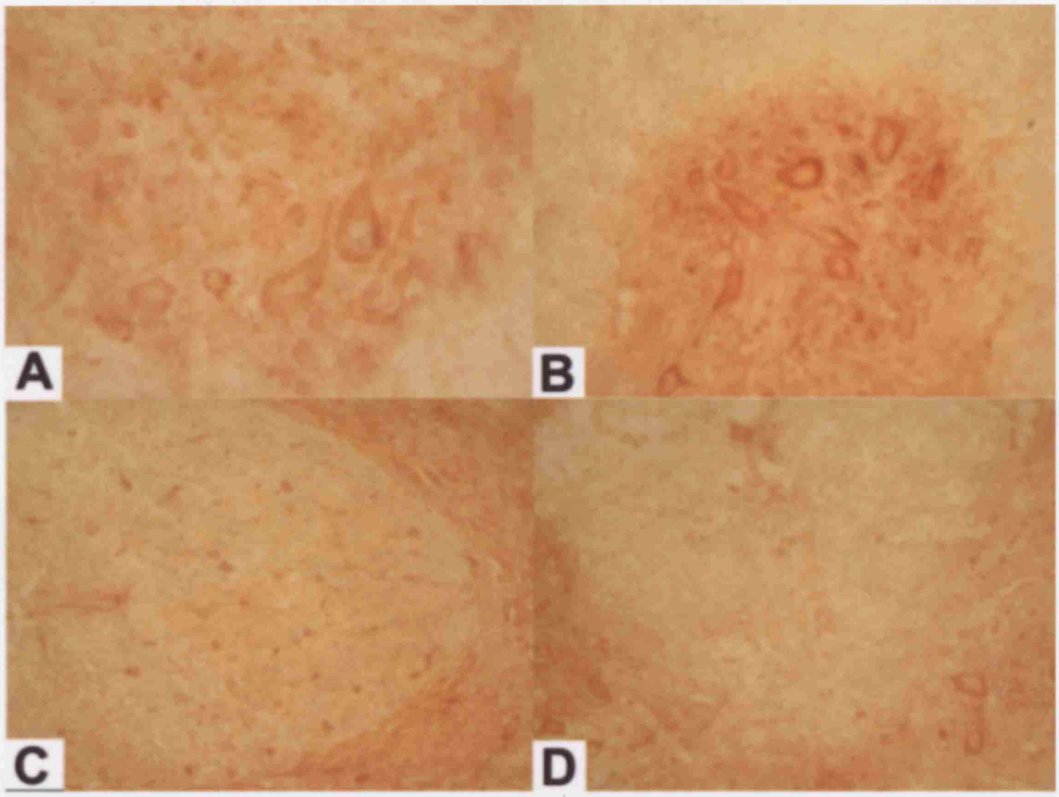

Plate 3. 1. Nogo-A Immunostaining in Wt Mice at 18 weeks.
A. Right Ventral Horn in Grey Matter, B. Left Ventral Horn in Grey Matter
C. Dorsal White Matter, D. Ventral White Matter

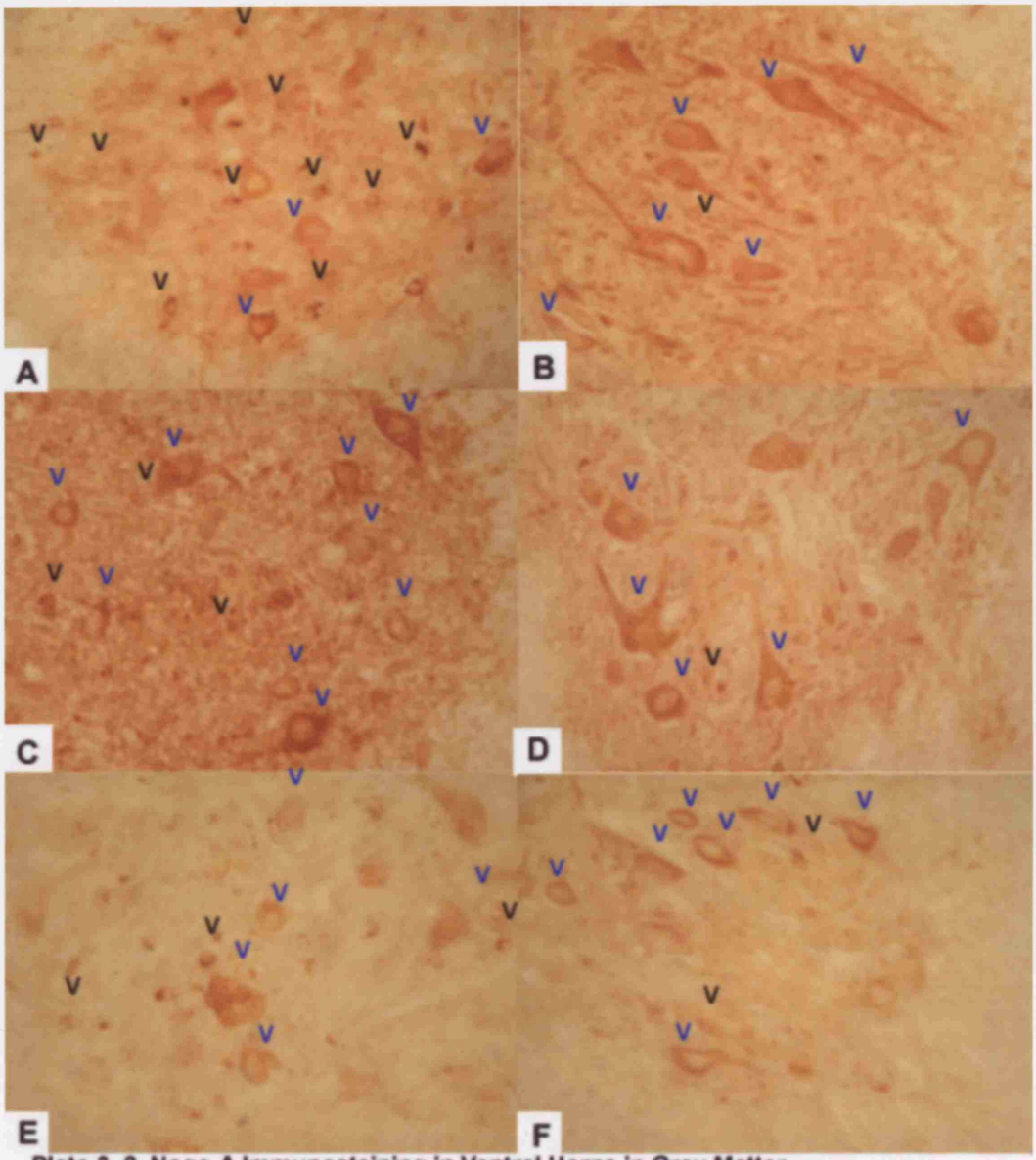

Plate 3. 2. Nogo-A Immunostaining in Ventral Horns in Grey Matter.
Increased Nogo-A immunoreactivity is illustrated in Ods of Tg animals during the clinical stage. Also, More Intense staining in neurons is demonstrated.
Blue arrows correspond to neurons and black arrows to Ods.
A-B. Clinical Stage (18 weeks): A. Tg and B. Wt.
C-D. Preclinical Stage (13 weeks): C. Tg and D. Wt.
E-F. Preclinical Stage (6 weeks): E. Tg and F. Wt.

Furthermore, there was an increase in Nogo-A stained Ods in the ventral white matter in Tg compared to Wt mice (Plate 3. 3) . Finally, the dorsal white matter showed increased levels of Nogo-A staining in Ods, but similar to that shown by Wt controls (Plate 3. 4).

GAP-43

Overall, GAP-43 pattern of immunostaining was diffused and scattered in the spinal cord sections and not as clear and straightforward as Nogo-A immunostaining. However, some discrete features were noticeably stained. The 6 weeks sample of both Tg and Wt did not show immunostaining and therefore were not analysed further. Generally, Tg mice demonstrated higher levels of immunoreactivity compared to Wt mice. Tg mice also demonstrated differences between the preclinical stage of 13 weeks and the clinical stage of 18 weeks; immunoreactivity at the preclinical stage was less than at the clinical stage, though this was variable from animal to animal.

Accordingly, the level of staining in Wt animals at the stage of 13 weeks was generally low and remarkably less, than in Tg at the corresponding age. In the photos of 13 weeks Tg mice, stained fibres going out of the ventral horn can be seen (Plate 3. 5). A fairly constant staining in the area of ventral CST in the ventral white matter was also observed. Finally, immunoreactivity could be seen in some neurons in the ventral horn.

Although the 18 weeks Tg mice showed variation in immunoreactivity, they demonstrated higher immunostaining levels comparing to the 18 weeks

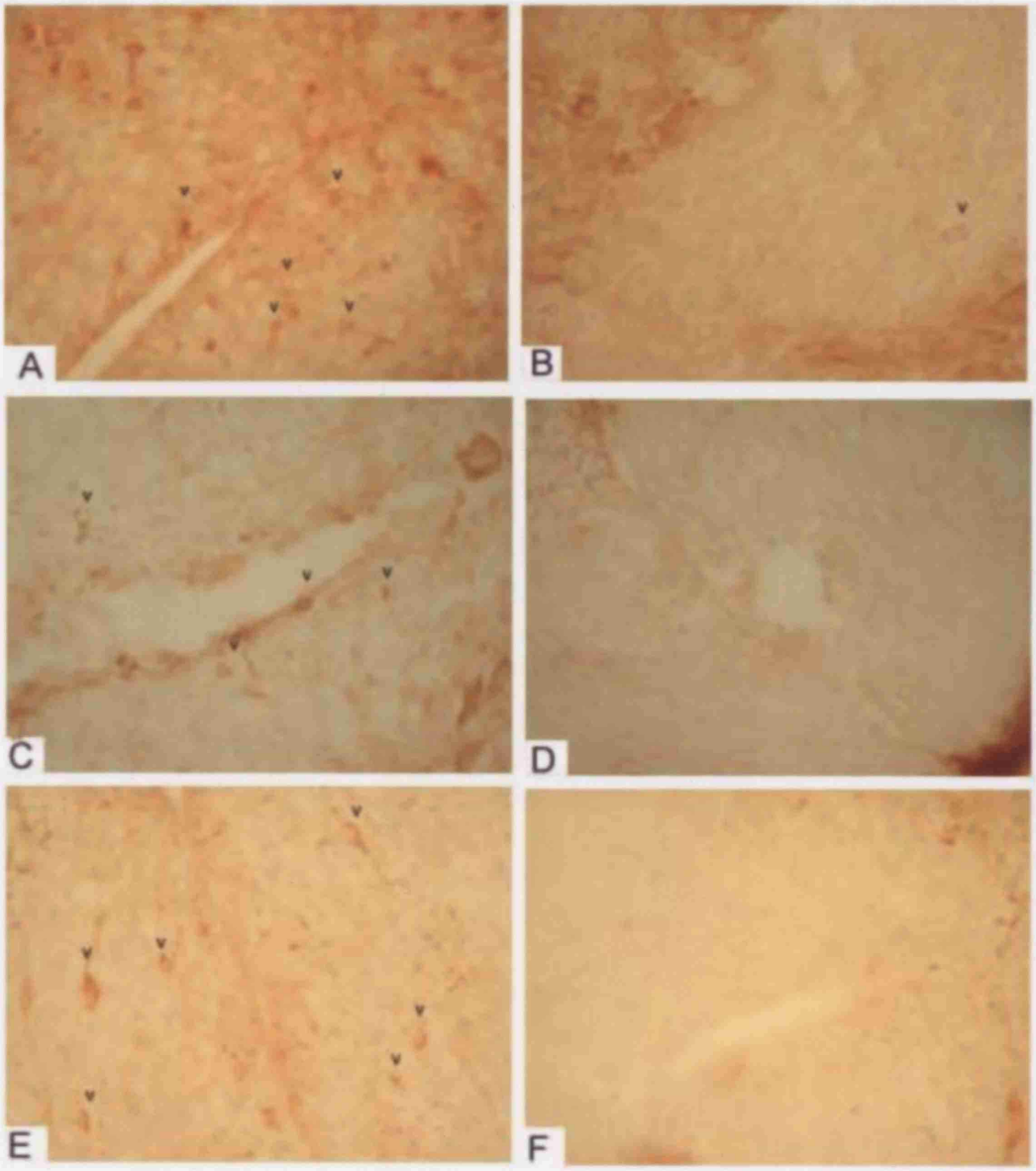

Plate 3. 3. Nogo-A Immunostaining in Ventral White Matter.
Increased Nogo-A Immunoreactivity is illustrated in Tg vs.Wt Animals During Clinical and Preclinical Stages.
A-B. Clinical Stage (18 weeks): A. Tg and B. Wt
C-D. Preclinical Stage (13 weeks): C. Tg and D. Wt
E-F. Preclinical Stage (6 weeks): E. Tg and F. Wt

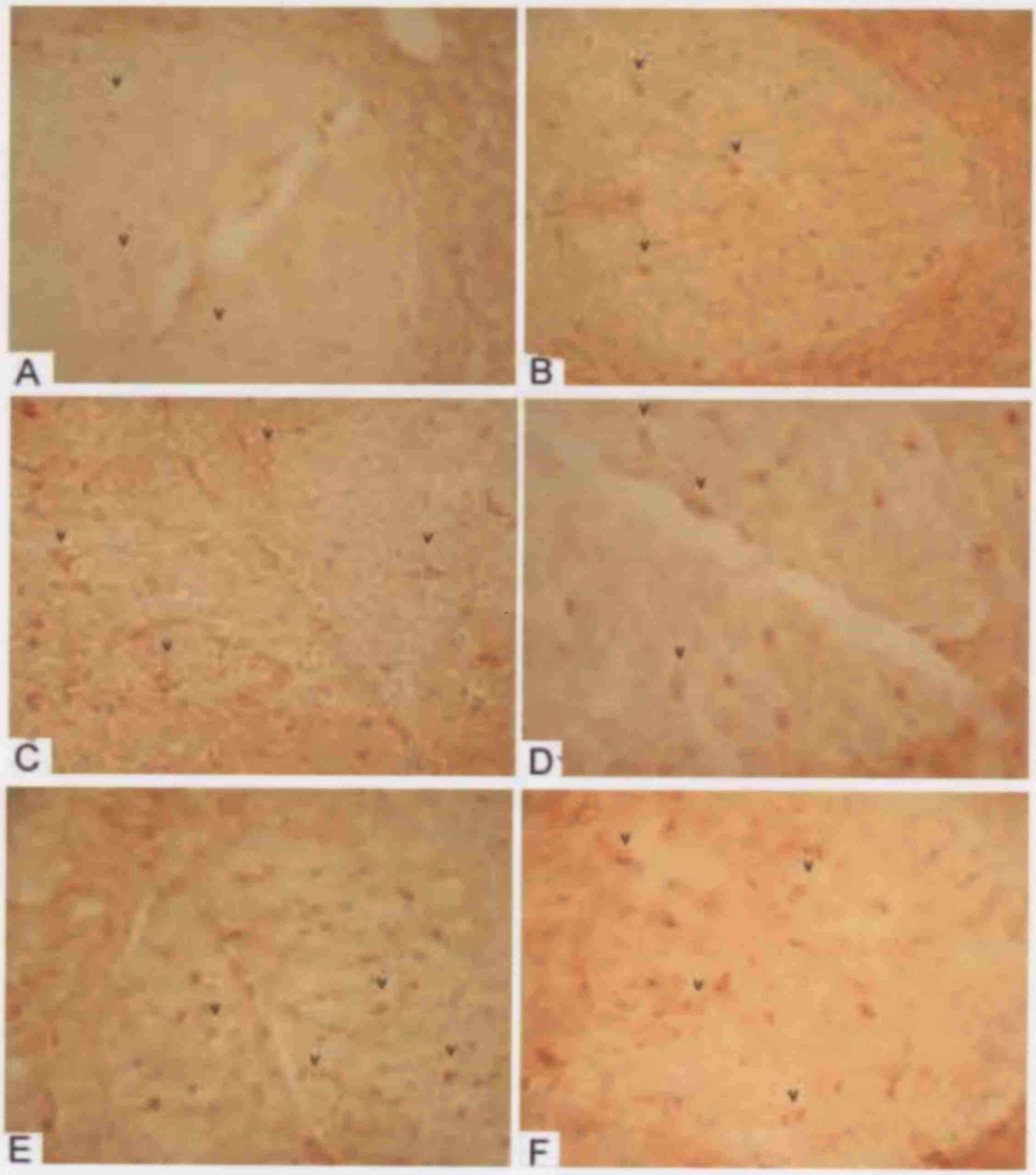

Plate 3. 4. Nogo-A Immunostaining in Dorsal White Matter. Similar Nogo-A Immunoreactivity is illustrated for both Tg and Wt Animals During Clinical and Preclinical Stages.
A-B. Clinical Stage (18 weeks): A. Tg and B. Wt
C-D. Preclinical Stage (13 weeks): C. Tg and D. Wt
E-F. Preclinical Stage (6 weeks): E. Tg and F. Wt

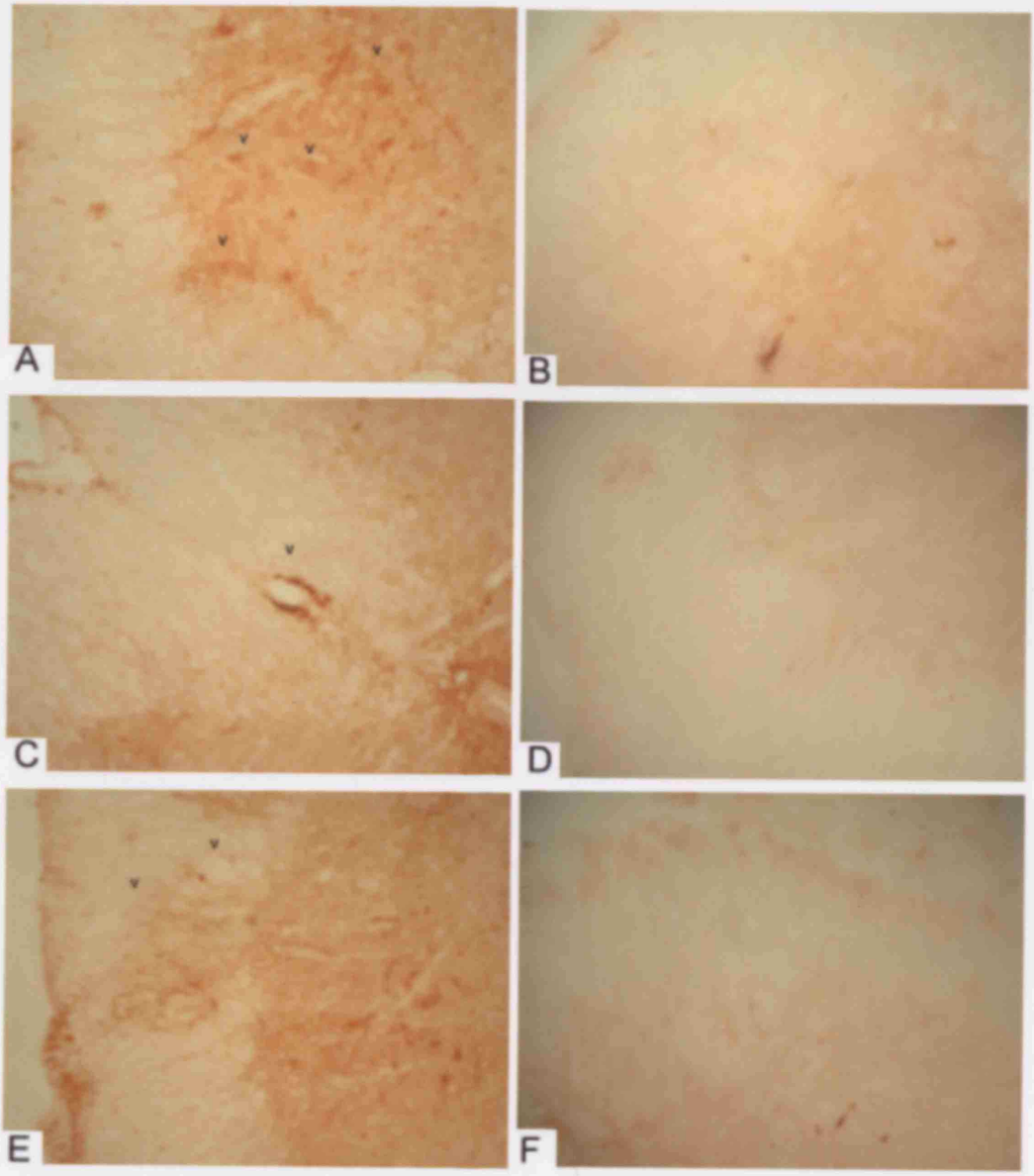

Plate 3. 5. GAP-43 Immunostaining in 13 weeks Preclinical Tg and Wt SOD1 mice.
Moderately Increased GAP-43 Immunoreactivity is illustrated in
Tg vs. Wt Animals during the Preclinical Stage (13 weeks).
A. Ventral Horn in Grey Matter of of a Tg mouse.
B. Ventral Horn of a Wt mouse of 13 weeks.
C. Ventral White Matter of a Tg mouse.
D. Ventral Horn Tip of a Wt mouse.
E. Ventral Horn of a Tg mouse.
F. Ventral White Matter of a Wt mouse.

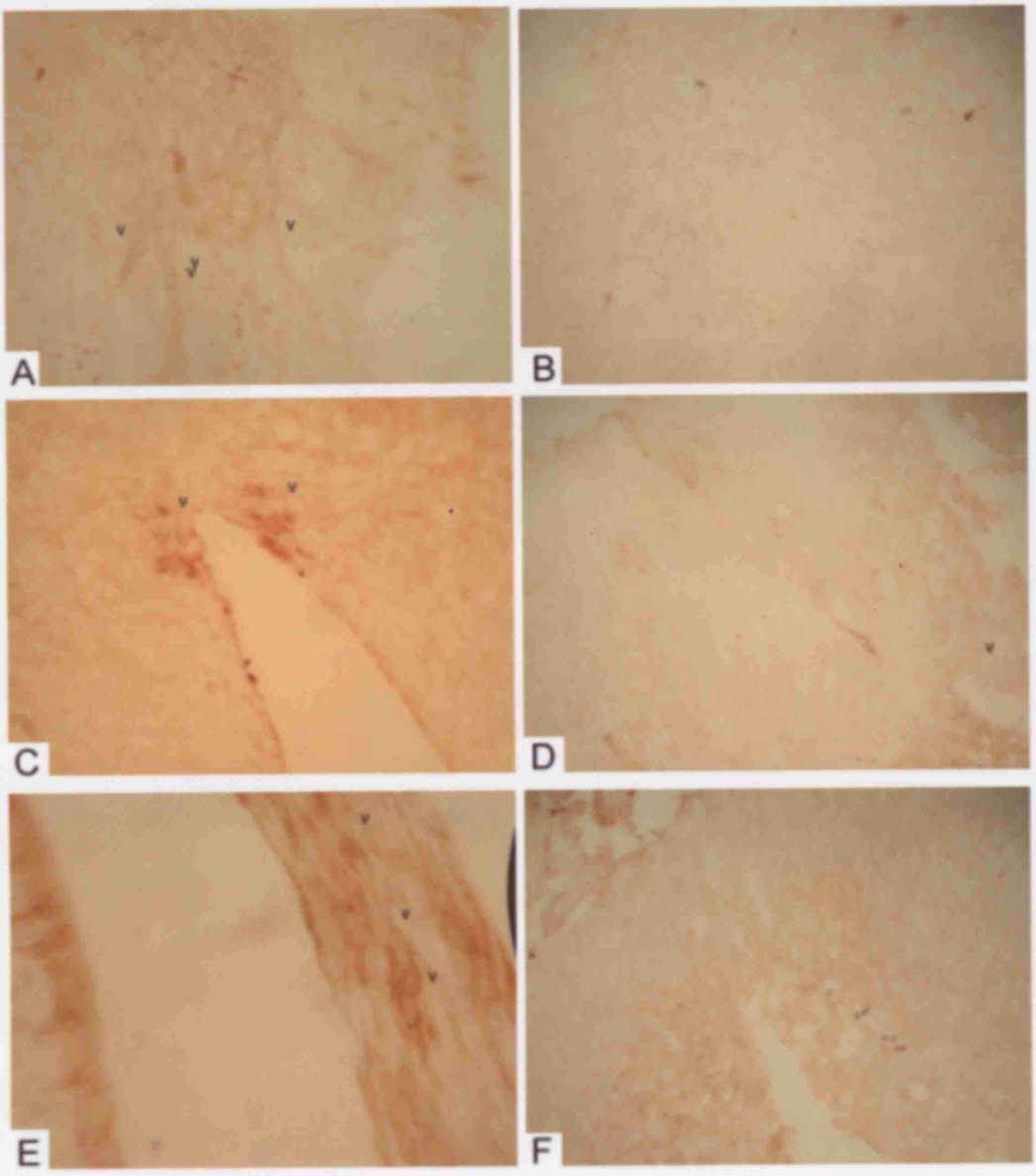

Plate 3. 6. GAP-43 Immunostaining in 18 weeks Clinical Tg and Wt mice. Increased GAP-43 Immunoreactivity is illustrated in Tg vs. Wt Animals during the Clinical Stage.
A. Ventral Horn in Grey Matter of a Tg mouse.
B. Ventral Horn of a Wt mouse of 13 weeks.
C. Ventral White Matter of a Tg mouse.
D. Ventral White Matter of a Wt mouse.
E. Ventral Root of a Tg mouse.
F. Dorsal White Matter of a Wt mouse.

Wt mice (Plate 3. 6). There was also immunoreactivity in motor neurons and in fibers coming out of the ventral horns, as observed also at the preclinical stage of 13 weeks. Finally, staining in ventral roots was detected. Wt animals showed no real staining during the clinical stage, consistent with the preclinical Wt pictures.

Quantitative Analysis of Nogo-A Immunoreactivity.

To further validate our qualitative observations, quantitative analysis was conducted on the photographs of sections stained with Nogo-A. Image analysis was performed with Photoshop and SigmaScan software as decribed in 'Methods'. Among the positive stained cells there were cells that were visible but did not demonstrate any staining. In order to be able to assess quantitatively the degree of staining, 4 random photos were chosen to give 3 standard average values, using the optical density tool of Photoshop software. An unstained, a stained and a heavily stained cell were randomly selected from each photograph and their average was calculated. Accordingly, these average values correspond to 3 different levels of staining density: unstained cells, stained cells and heavily stained cells and are illustrated in Table 3.2. Most importantly, throughout the experiments, the difference in average background 'staining' was negligibly small (mean 71.67, standard deviation 2.77) and therefore background variation was not a factor in any variation in staining intensity found between neurones and oligodendrocytes groups in Wt and Tg mice of different ages.

	UNSTAINED	STAINED	HEAVILY STAINED
F#3-2-L	8.67	16.67	22.01
R#6-1-R	10	14.34	25
B#1-2-R	6.67	18.67	19.34
D#5-1-R	9.67	17.34	38
AVERAGE	8.7525	16.755	26.0875

Table 3. 2. Classification of Staining Density Values in 3 Categories Depending on the Level of Staining Density of the Cell.

Ods in Ventral Horns of Tg Mice Showed Greater Nogo-A Immunoreactivity.

The data in Figure 3. 1 show that increased number Ods were stained in the ventral horn of 18 weeks transgenic animals. Specifically, the number of immunostained ods in clinical stage is 0.28/1000μm^2 which makes a remarkable difference in contrast to the levels of the preclinical stages of 13 and 6 weeks (t-test, p=0.0030 and 0.0045 respectively). Tg animals of 13 and 6 weeks show similar levels of stained ods. In particular, their values of stained Ods/1000μm^2 at these stages are 0.14 and 0.13 respectively which are half of the mean number of stained Ods found at 18 weeks.

Wt mice show similar levels of stained Ods in ventral horn grey matter at all stages, albeit with a slight decrease in 13 weeks. The values of Wt animals range from 0.15 at 18 weeks, 0.1 at 13 weeks and 0.15 at 6 weeks of age. In comparison, the main difference between Tg and Wt animals is in the clinical stage of 18 weeks (t-test; p=0.0074); Tg mice show nearly double the response in Nogo-A immunoreactivity, whereas Wt immunoreactivity at 18 weeks remains at the same levels as at the preclinical stages of 13 and 6 weeks.

Figure 3. 2 shows the mean values of the number of immunostained Ods/1000 μm^2 in ventral horn grey matter of Tg mice at the age of 18 weeks. The figure also shows a degree of variation between the mice. Specifically, two mice, B#1 and JAX#A2, have a high level of stained OD/1000 μm^2 with the values of 0.4 and 0.33 respectively.

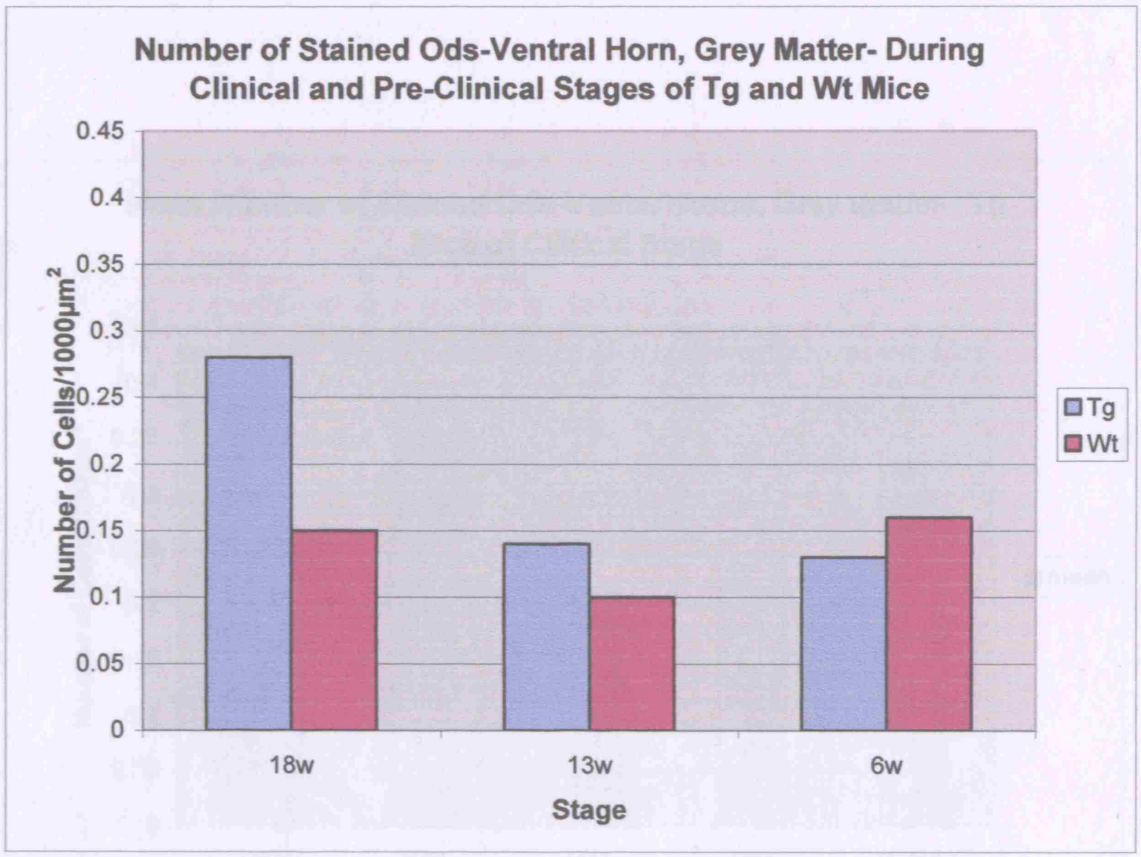

Figure 3. 1. The Data Represent Means of the Number of Stained Cells/1000 µm² for Tg vs. Wt Mice of 18 (Clinical), 13 and 6 (Preclinical) Weeks of Age.

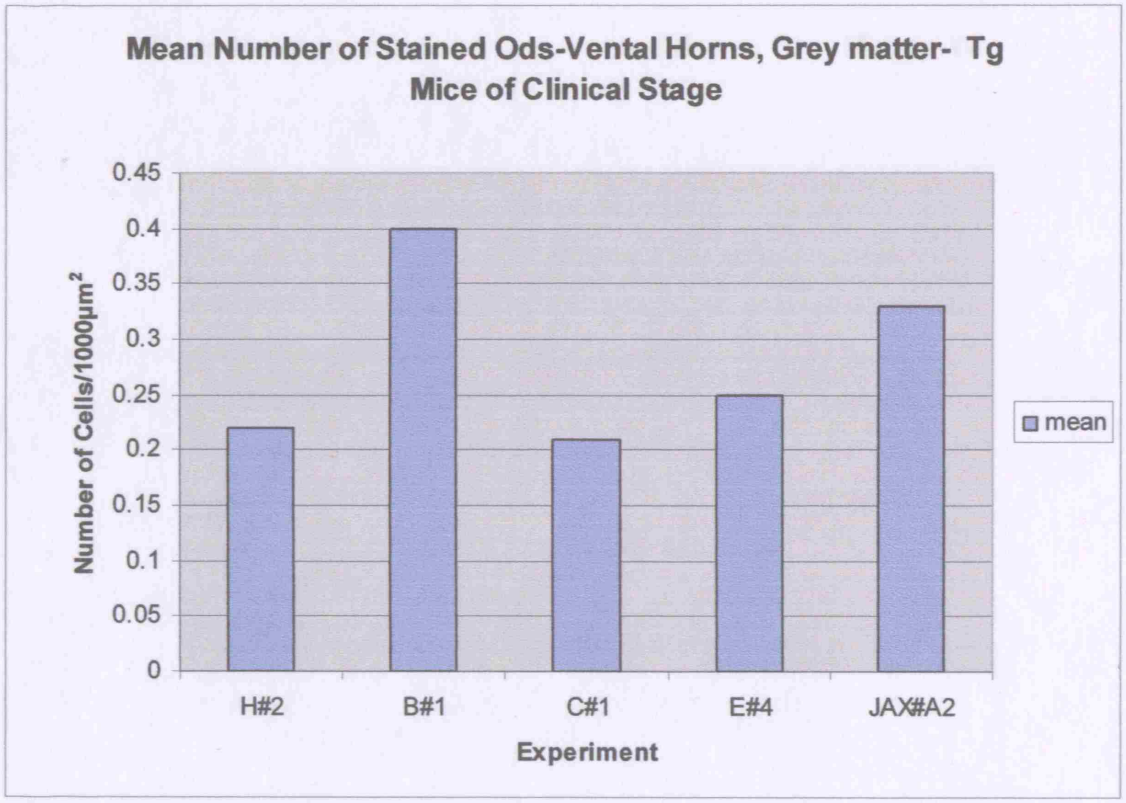

Figure 3. 2. The Data Represent the Means of the Number of Stained Ods/1000 μm^2 in Ventral Horn- Grey Matter of 18w Tg mice.

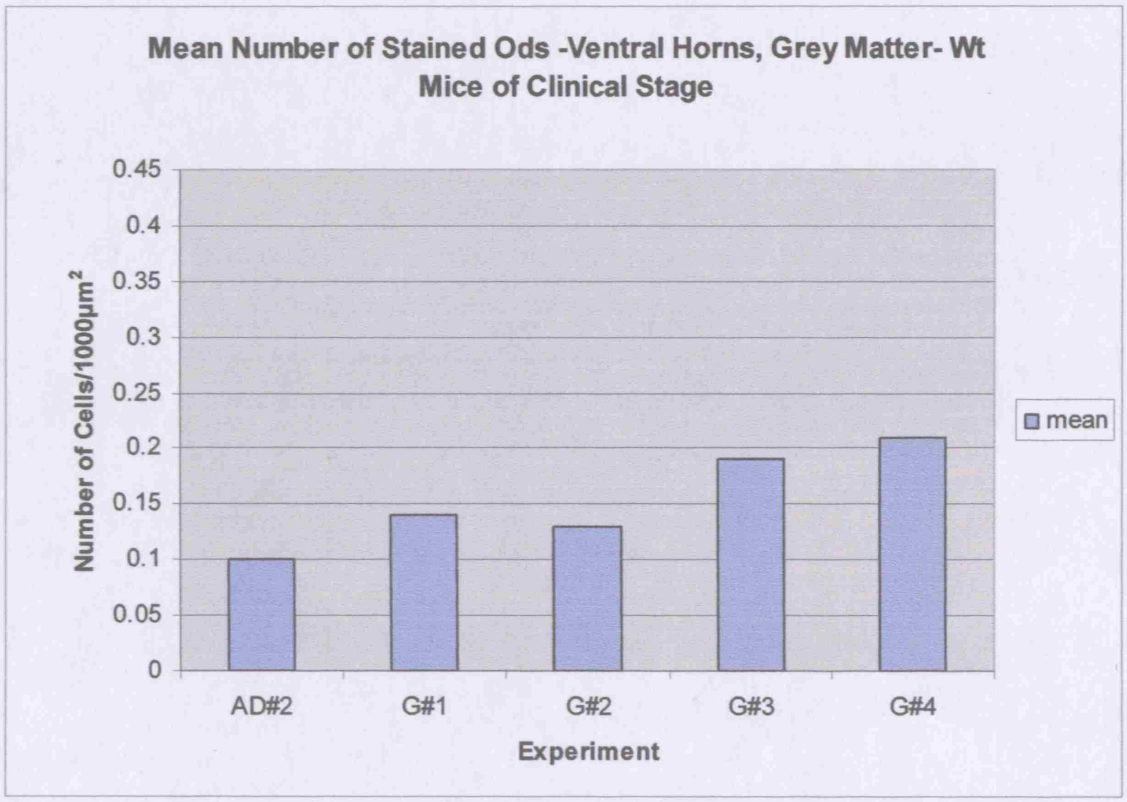

Figure 3. 3. The Data Represent the Means of the Number of Stained Ods/1000 μm^2 in Ventral Horn, Grey Matter of 18 Weeks Wt Mice.

The level of stained Ods for the three other animals indicates less variation, with values ranging between 0.22 and 0.25.

On the other hand, Figure 3. 3 shows that the mean values of the number of stained Ods/1000 μm^2 of 18 weeks Wt mice have a smaller variation in values, ranging between 0.1 and 0.21. What is notable here is that the higher values of Wt animals (G#3 and G#4) which are 0.19 and 0.21 respectively are equivalent to the lowest values of Tg animals. The three other mice of the sample show values that remain below 0.15.

The Figure 3.4 illustrates the mean values of stained Ods/1000 μm^2 in ventral horns in grey matter of 6 weeks Tg mice. Here, the degree of variation is very much lower than that illustrated in the Figure 3.2 for Tg mice of 18 weeks. The lowest value, that both Q#8 and R#8 show, is 0.11 Ods/1000 μm^2, though the highest value (R#7) is 0.16 OD/1000 μm^2.

The levels of stained cells in this figure come in contrast to the levels of stained cells of Figure 3. 2, indicating a different extent of immunoreactivity between the clinical stage of 18 weeks and the preclinical of 6 weeks (t-test; p=0.0045).

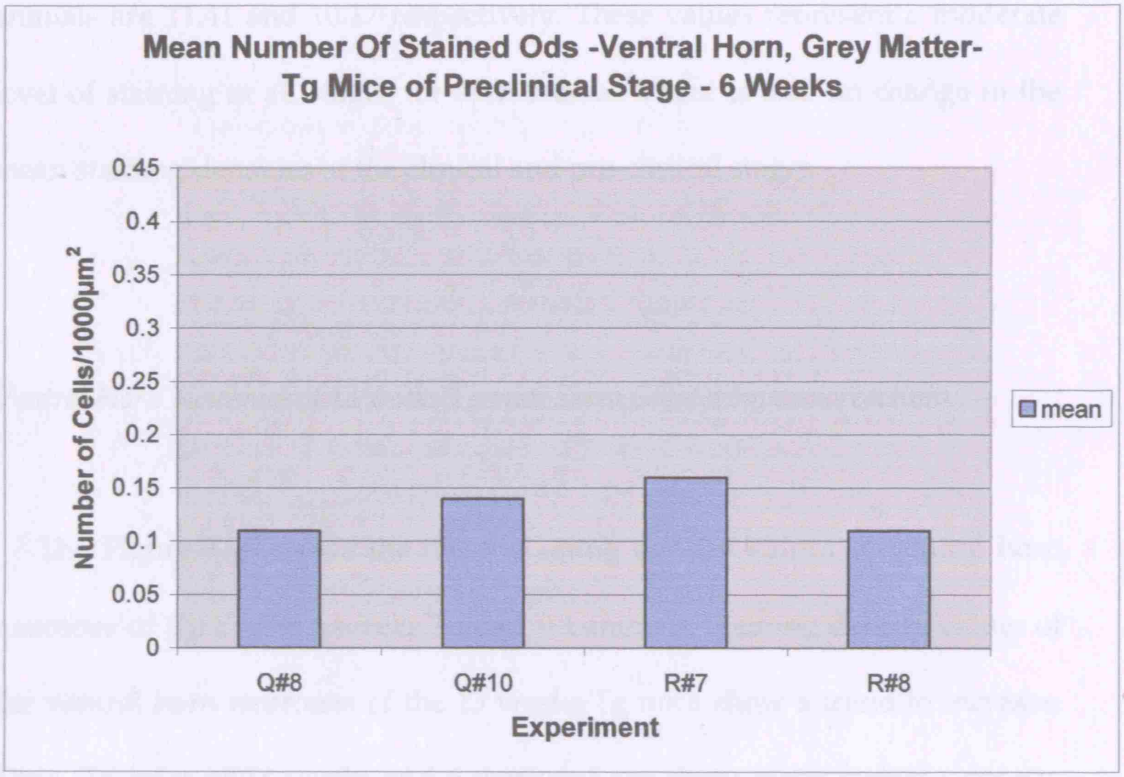

Figure 3. 4. The Data Represent the Means of the Number of Stained Ventral Horn Ods/1000 µm² of the Preclinical 6 Weeks Tg Mice.

The data in the Figure 3.5 show that the staining density varies in equal amounts. In particular, the 18 weeks Tg and Wt mice show staining density values of 11.21 and 9.48 respectively; the values of 13 weeks Tg and Wt mice are 12.49 and 11.68 respectively and, finally, the values of 6 weeks Tg and Wt animals are 11.41 and 10.17 respectively. These values represent a moderate level of staining at all stages for each animal. There is also no change in the mean staining densities at the clinical and pre-clinical stages.

Ventral Horn Neurones of 13 weeks Tg mice Show Greater Immunoreactivity.

The Figure 3. 6 shows the mean staining density values of ventral horn neurones of 18, 13 and 6 weeks Tg and Wt animals. Staining density values of the ventral horn neurones of the 13 weeks Tg mice show a trend to increase. Thus, Tg mice of 18 weeks and 6 weeks of age show mean staining density values of 10.56 and 11.21 respectively, while 13 weeks Tg mice respective values extend to 15.24. It can be noticed then a significant difference in immunoreactivity between the preclinical stage of 13 weeks and the clinical stage of 18 weeks in Tg mice (t-test; $p= 0.0273$), but also between the preclinical stages of 13 weeks and 6 weeks (t-test; $p=0.037$) with a notable increase in 13 weeks Tg animals. However, the Tg vs. Wt mice staining density values did not demonstrate significant differences.

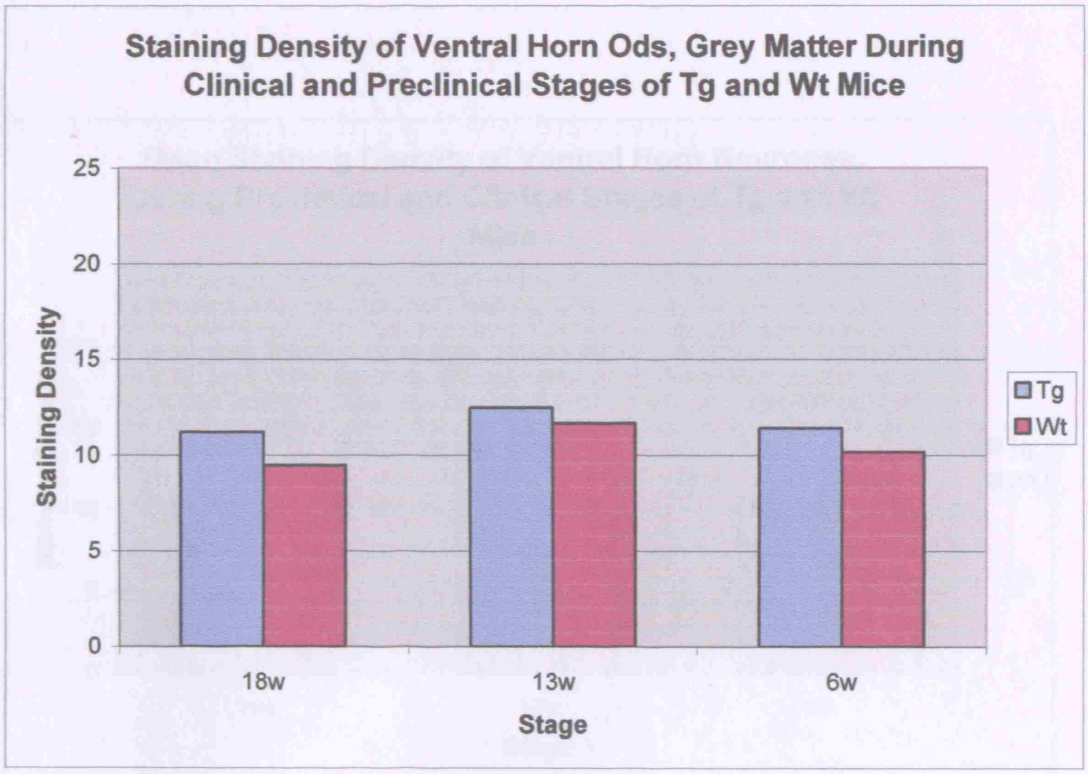

Figure 3. 5. The Data Represent Mean Staining Densities of Ods in Ventral Horns in Grey Matter of 18 (Clinical), 13 and 6 (Preclinical) Weeks Tg and Wt Mice.

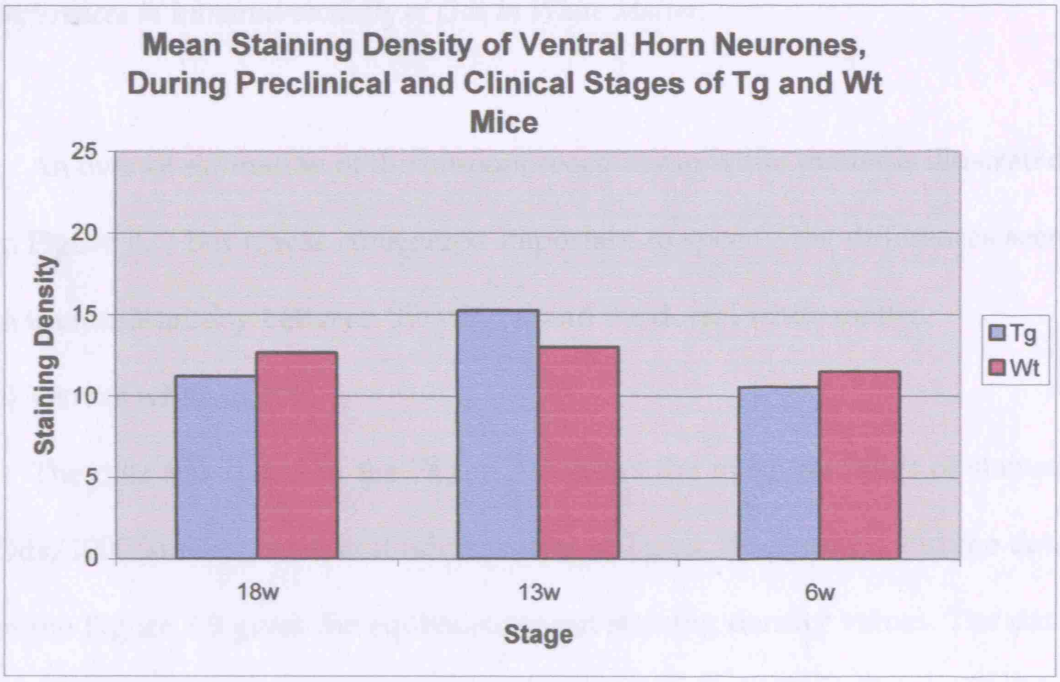

Figure 3. 6. The Data Represent the Mean Staining Density of Ventral Horn Neurones of 18 (Clinical), 13 and 6 (Preclinical) Weeks Tg and Wt mice.

The mean levels of staining density in ventral horn neurones of Wt mice have a similar range of values. Specifically, the mean values are 11.5 for 6 weeks, 13.1 for 13 weeks and 12.67 for 18 weeks. These results indicate that the levels of staining density of Wt mice of each stage remain more or less equivalent.

Differences in Immunoreactivity of Ods in White Matter.

An overall estimation of the immunoreactivity in white matter is illustrated in Figure 3. 7 but it was considered important to specify the differences seen in immunostaining between the ventral and the dorsal white matter.

a) Ventral white matter

The data illustrated in the Figure 3.8 shows the mean numbers of stained Ods/1000 μm^2 in the ventral white matter of Tg vs. Wt animals, and the data in the Figure 3.9 gives the equivalent mean staining density values. The data demonstrate a general increase in Tg mice Nogo-A immunoreactivity in ventral white matter compared to the Wt mice sample (18w Tg vs. 18w Wt, p=0.0012, 13w Tg vs. 13w Wt, p=0.0055, 6w Tg vs. 6 w Wt, p=0.0034).

Tg mice of 18 weeks and 6 weeks show similar levels of numbers of stained Ods/1000 μm^{22} (0.21 and 0.25 respectively) and also in staining density (12.76 and 10.83 respectively). In the stage of 13 weeks, Tg animals show a slight decrease in numbers of stained Ods/1000 μm^2 (0.18) but greater mean staining density (15.22).

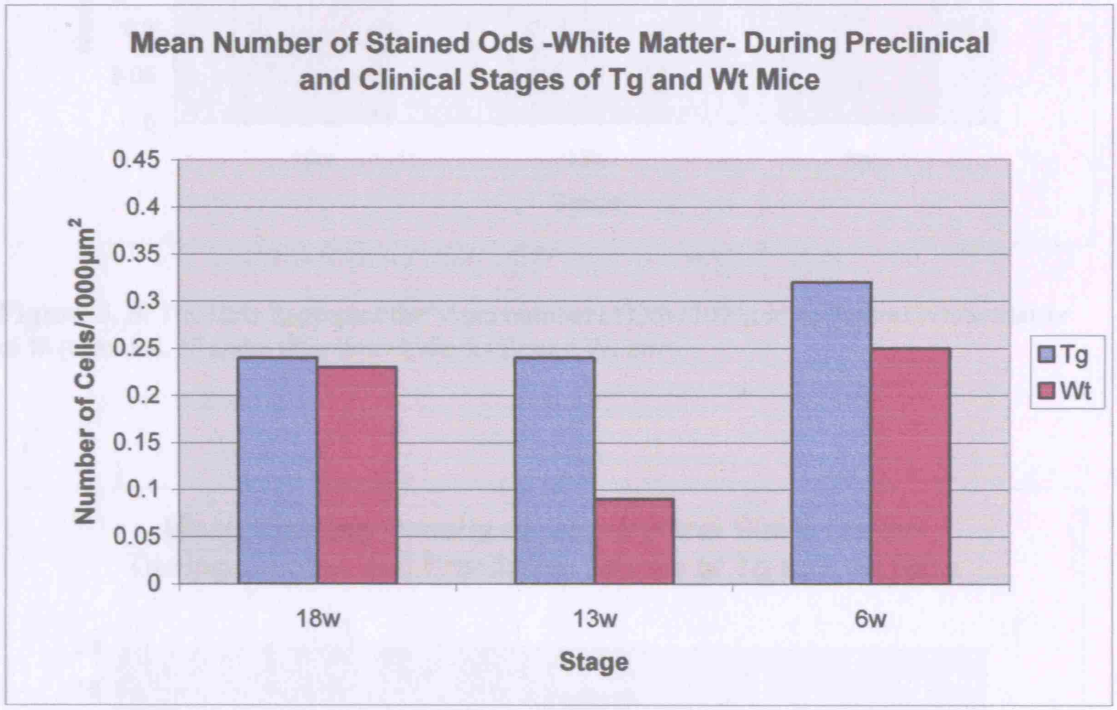

Figure 3. 7. The Data Represent the Mean number of Stained Ods/1000µm² in White Matter of 18 (Clinical) and 6, 13 (Preclinical) weeks Tg and Wt Mice.

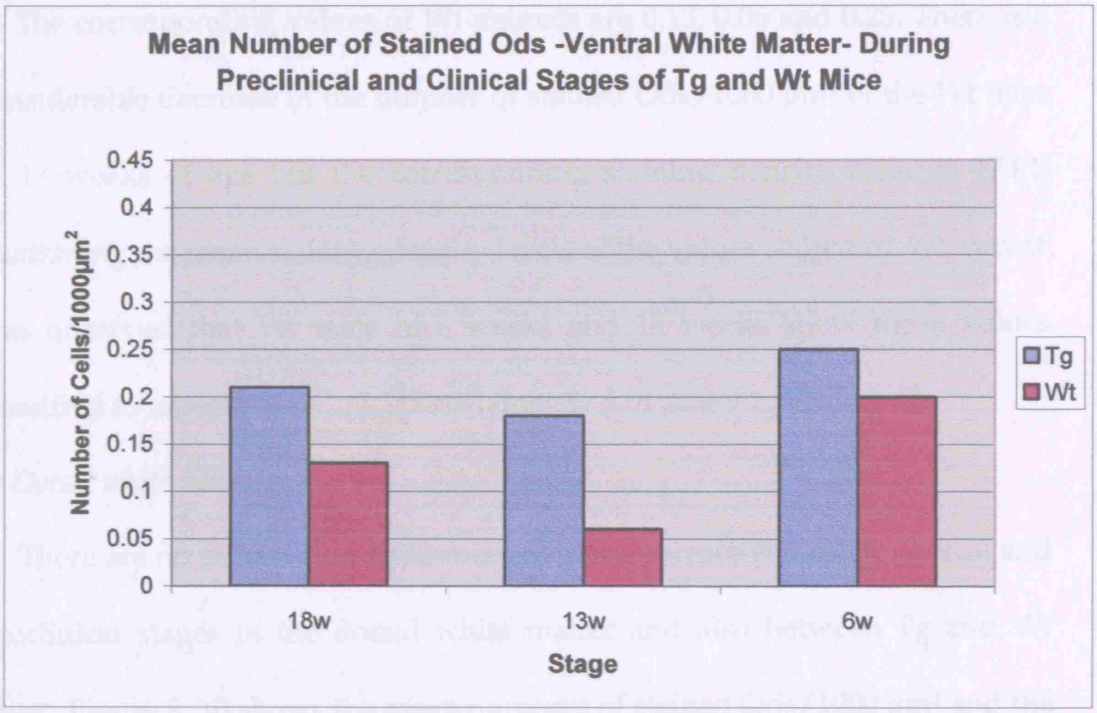

Figure 3. 8. The Data Represent the Mean number of Ods/1000µm² in Ventral White Matter of 18 (Clinical), 13 and 6 (Preclinical) weeks Tg and Wt mice.

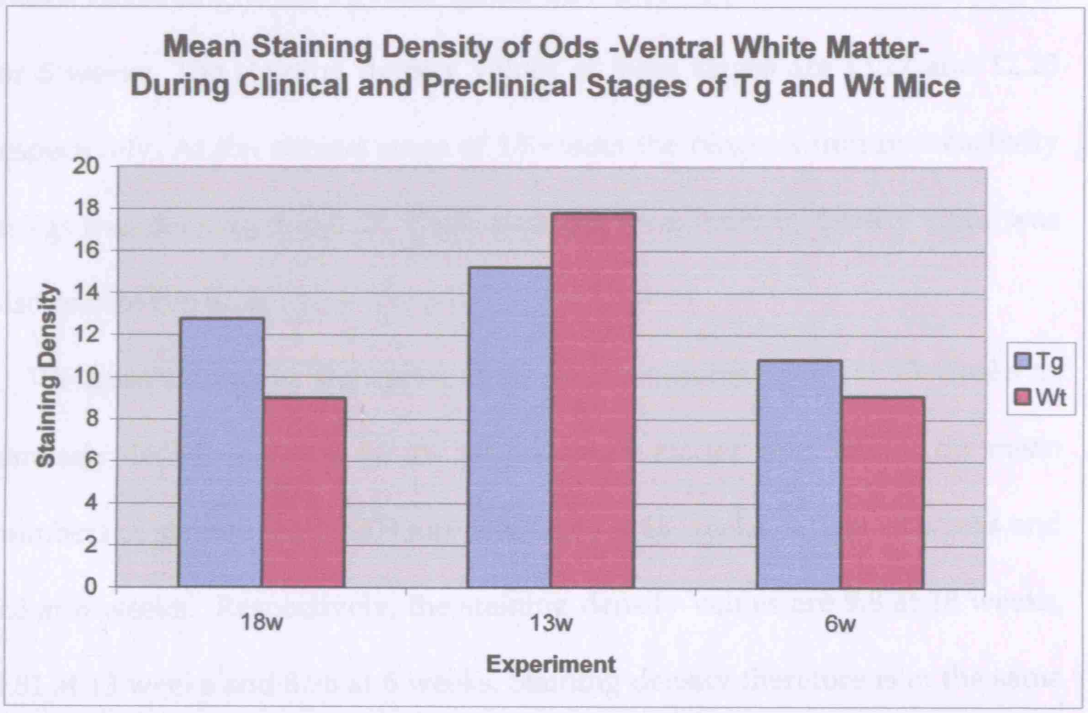

Figure 3. 9. The Data Represent the Mean staining density rates in Ventral White Matter of 18 (Clinical), 13 and 6 (Preclinical) weeks Tg and Wt mice.

The corresponding values of Wt animals are 0.13, 0.06 and 0.25. There is a considerable decrease in the number of stained Ods/1000 μm^2 of the Wt mice of 13 weeks of age but the corresponding staining density value is 17.81. Examining the mean staining density levels of the values shown by Wt mice it was observed that Wt mice of 6 weeks and 18 weeks show mean values classified to unstained to low stained density 9.01 and 9.1 (Table 3. 2).

b) Dorsal white matter

There are no remarkable differences in immunoreactivity at the clinical and preclinical stages in the dorsal white matter and also between Tg and Wt mice. Figure 3. 10 shows the mean numbers of stained Ods/1000 μm^2 and the Figure 3. 11 shows the staining density of dorsal white matter of Tg and Wt mice at the clinical stage of 18 weeks and at the preclinical stages of 13 and 6 weeks. Accordingly, the Tg mice values extend to 0.3 for 13 weeks and to 0.39 for 6 weeks. The staining density values at these stages are 13.27 and 12.23 respectively. At the clinical stage of 18 weeks the Nogo-A immunoreactivity in Tgs was decreased in 0.27. Their corresponding staining density value was also reduced in 9.28.

Wt animals' values showed a curve in immunoreactivity at 13 weeks as similarly described above for the ventral white matter. Specifically, the mean numbers of stained Ods/1000 μm^2 were 0.34 at 18 weeks, 0.12 at 13 weeks and 0.3 at 6 weeks. Respectively, the staining density values are 9.8 at 18 weeks, 9.81 at 13 weeks and 8.96 at 6 weeks. Staining density therefore is in the same level at all stages.

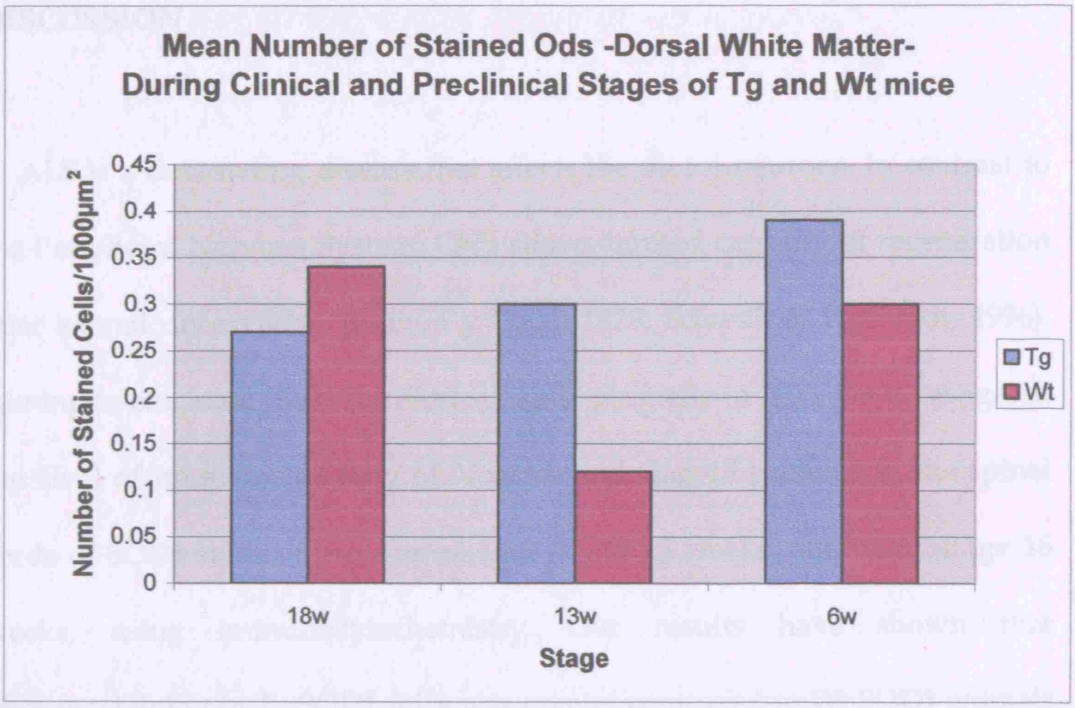

Figure 3. 10. The Data Represent the Mean number of Ods/1000µm² in Dorsal White Matter of 18 (Clinical), 13 and 6 (Preclinical) weeks Tg and Wt mice.

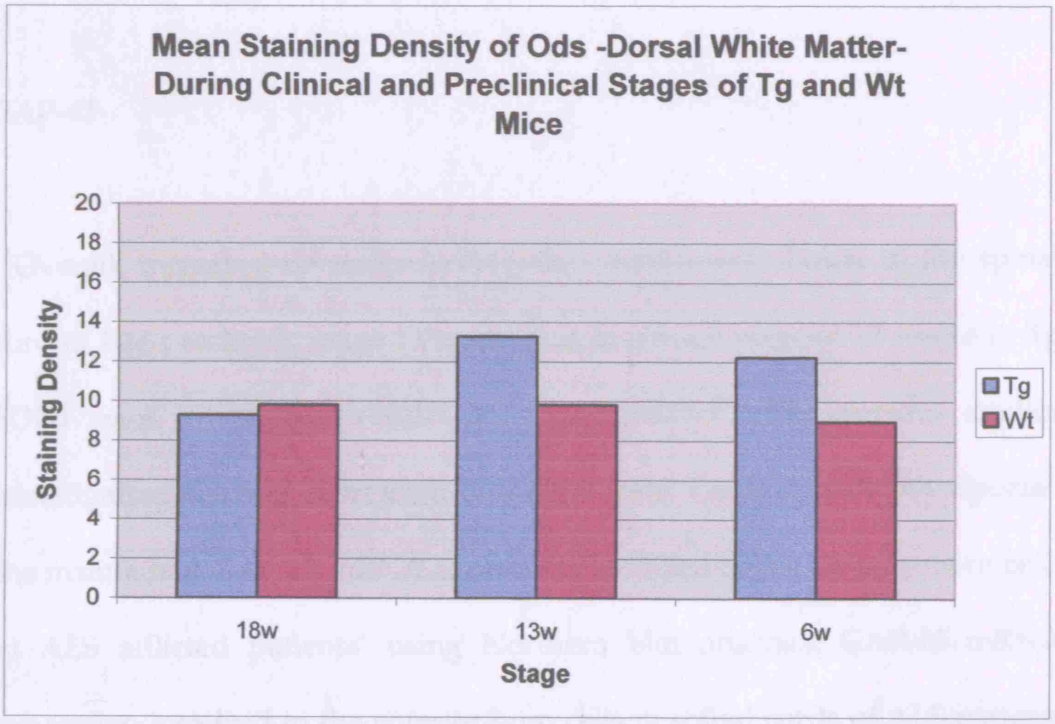

Figure 3. 11. The Data Represent the Mean Staining Density Rates in Dorsal White Matter of 18 (Clinical), 13 and 6 (Preclinical) weeks Tg and Wt mice.

DISCUSSION

ALS is a devastating disease that affects the motor neurons. In contrast to the Peripheral Nervous System, CNS shows limited capacity of regeneration after axonal denervation (Ramon y Cajal, 1928, Schwab & Bartholdi, 1996). Aiming to elucidate the features of synaptic plasticity in ALS, we investigated the level of immunoreactivity of Nogo-A and Gap-43 proteins in the spinal cords of SOD1 mice of pre-clinical ages 6 and 13 weeks, and clinical age 18 weeks, using immunocytochemistry. Our results have shown that immunostaining in Tg SOD1 mice was greater compared to Wt SOD1 animals for both proteins Nogo-A and GAP-43 confirming our hypothesis of altered immunoreactivity of those two proteins during ALS.

GAP-43

Overall, increased immunoreactivity in GAP-43 was shown in the spinal cord of late preclinical stage 13 weeks and in clinical stage of 18 weeks in Tg SOD1 mice. These results are in accordance with previous studies investigating GAP-43 expression in mRNA level. Clark *et al.* (1990) reported the maintained GAP-43 mRNA expression localized to the anterior horn cells in ALS afflicted patients' using Northern blot analysis. GAP-43 mRNA expression localized to the anterior horn cells in spinal cords of ALS patients was also evaluated by Parhad *et al.* (1992) using in situ hybridization (ISH) to

assess whether surviving neurons can mount an appropriate response to injury. Finally, Kage *et al.* (1998) underlined that the abnormal expression of GAP-43 mRNA is due to a quantitative increase of the protein expression.

Such evidence suggests a regeneration attempt is likely to happen during ALS. The increase in GAP-43 immunoreactivity indicates that the mechanism which leads to degeneration in ALS does not necessarily compromise the neuron's capacity for expression of growth-associated proteins. It remains to be detected whether this abnormal GAP-43 expression is just a response to the degeneration in ALS. In particular, the increase in GAP43 may reflect either a beneficial or detrimental part of the pathogenic process in ALS. Sustained GAP-43 expression may be damaging to the neuron via a maintained high level of metabolism, but there is currently no direct evidence to this effect in ALS. If this GAP-43 increase is part of a reaction ton the disease, at the later stages we would observe a mass GAP-43 immunostaining accumulated from earlier preclinical stages. However, this does not appear to have happened in this study, suggesting the role of this abnormal GAP-43 increase is more complicated.

Indeed, GAP-43 increased expression consists only a part of the overall alteration in synaptic plasticity during ALS. In recent immunohistochemical studies (Ikemoto & Hirano, 1996, Ikemoto *et al.*, 1994, Ikemoto *et al.*, 1996, Matsumoto *et al.*, 1994, Sasaki & Maruyama, 1994), alterations of the axonal terminals of the afferent fibres (presynaptic terminals), have been investigated using antibodies against synaptophysin (SYP), a glycoprotein which is a

component of the membrane of presynaptic terminal vesicles. Such studies revealed a degeneration of the presynaptic terminals from the afferents and synaptic alterations possibly associated with plasticity involving synapses of pre-motor pathways.

Thus, a reaction seems to occur during the disease reflected by alterations in synaptic organisation and neurite regeneration, but finally the degeneration in the later stages seems to overcome attempt. Time constraints prevented the quantitative analysis of our results because the pattern of GAP-43 immunoreactivity was complex, and not easily measurable using the methods applied to analyse Nogo. In the future, maybe design of an appropriate method for examining patches of GAP-43 immunoreactivity will support the observations discussed above.

Nogo-A

Nogo-A immunostaining was detected in all SOD1 mice, both in Wt and Tg, but was increased in grey matter Ods of 18 weeks Tg mice. In addition, Nogo-A immunostaining was moderately more intense in ventral horn neurones of the 13 weeks SOD1 mice. In white matter tissue, Tg SOD1 mice also demonstrated increased Nogo-A in the ventral division at all stages, though in the dorsal part immunoreactivity was constantly increased for all animals at all stages.

Nogo-A labelling was on the whole strong and clear in the neurones and Ods of the spinal cord. It was also noticeable that some neuronal and glial cell bodies were devoid of Nogo-A staining. Nogo-A negative neurons and Ods could also be found scattered amongst the Nogo-A positive clusters. These results further illustrate the specificity of the antibody labelling and indicate that Nogo-A is expressed normally only in a proportion of ventral horn cells.

Additionally, Nogo-A seems to be well distributed in our control sample. This is in accordance with previous studies in which the expression pattern of Nogo-A in normal tissue was examined (Josephson *et al.*, 2001, Liu *et al.*, 2002, Huber *et al.*, 2002, Buss *et al.*, 2005) suggesting that the underlying biological role of the protein is not exclusively pathological. Accordingly, Josephson *et al.* (2001) conducted an in situ study which has demonstrated widespread expression of Nogo mRNA in the foetal, developing, and adult nervous system of rat and man. Liu *et al.* (2002) examined the staining in ventral grey matter of the mouse spinal cord and motor neurons and their results demonstrated Nogo-A immunoreactivity in these areas. Huber *et al.* (2002) has also shown the widespread localisation of Nogo-A in the CNS. Finally, in the study of Buss *et al.* (2005) in human adult nervous system, the spinal cord tissue was 80% stained. In our study, there was analogous distribution of Nogo-A at the ventral spinal cord grey and white matter in Wt animals at all stages and therefore were similar opposing to the levels in Tg SOD1 mice. These results are further explained below.

Increased Nogo-A Staining in Ventral Grey Matter Ods in SOD1 Tg mice During Clinical Stage.

One of the main findings of this study was the enhancement of immunoreactivity of Nogo-A in the ventral grey matter Ods of the 18 weeks SOD1 mice. Tg SOD1 mice of 18 weeks show clinical symptoms (hindlimb weakness and muscle wasting) similar to those shown by patients affected by ALS (Wong *et al.*, 1995, Bruijn *et al.*, 1997). Nevertheless, a large variability of Nogo-A was observed in the numbers of stained Ods among the 18 weeks SOD1 sample. This can be explained by the fact that individual animals show slight chronological dissimilarities in terms of the onset and the progression of the clinical symptoms, which may extend to differences seen in Nogo-A.

Increased Nogo-A immunoreactivity in Ventral White Matter of SOD1 Tg Mice..

A higher level of Nogo-A labelling was also observed in the ventral white matter of the SOD1 sample. In general, the ventral white matter is the part of spinal cord where a mixture of ventral corticospinal tract axons descend and ventral roots project from motor neurons to their target muscles. Increased immunoreactivity of Nogo-A in this area can possibly be an indication of axonal inhibitory activity. However, it was not clear from the data whether this increase is related to disease progression in the mice. A developing increase of Nogo-A immunoreactivity during the different stages was not directly observed, which would be likely to happen if the staining of Ods in this area is related with inhibitory axonal regeneration activity. This may

become more evident if future studies examined a larger samples of animals at each age.

There was also a considerable decrease in Nogo-A staining in white matter of 13 weeks Wt mice. This difference probably reflected technical problems in two experiments, E#5 and K#1, which unfortunately were impossible to repeat because of the restriction of time. E#5 showed very low immunostaining, allowing only the identification of the larger cells and K#1 had quite damaged tissue, so sampling was restricted to 2 sets of photographs instead of 3. It is therefore believed that the mean values presented for the 13 weeks Wt sample in white matter were artifactually low relative to the values presented for the other stages because of the reasons described above.

Increased Nogo-A immunoreactivity in Dorsal White Matter.

Increased Nogo-A staining in dorsal white matter was a general picture both for Wt and Tg animals and possibly can be related to a physiological role of Nogo-A in this area. This result is consistent with that of Buss *et al.* (2005) who showed micrographs of white matter in the spinal cord of adult human sample stained with Nogo-A, but it was not specified whether it was dorsal or ventral. However, it is unclear from the literature whether Nogo-A is associated with axonal plasticity in this area, and the expression of the protein here may be only indirectly associated with the motor function.

Increased Nogo-A Immunostaining in Ventral Horn Neurones of 13 weeks SOD1 Mice.

What is also derived from the data is the increase of Nogo-A immunoreactivity in the ventral horn neurones of the preclinical 13 week SOD1 mice. Nogo-A staining in neurones is not a novel finding. Previous studies (Josephson *et al.*, 2001; Liu *et al.*, 2002; Buss *et al.*, 2005; and Huber *et al.*, 2002) demonstrate that Nogo-A is expressed in CNS neurones. Thus, Nogo-A is both expressed in Ods and in the cell body of the larger neurones.

The exact function of Nogo-A in neurons is unknown. It has been suggested by the authors of the studies cited above, that neuronal Nogo-A may have an endogenous function(s) that either may be or not related with its ability to inhibit neurite growth. Accordingly, Nogo-A is intracellularly expressed in a reticular pattern (GrandPre´ *et al.*, 2000), as are the other isoforms of Nogo, the -B and –C, and other members of the RTN family of proteins (van de Velde et al., 1994) to which Nogo isoforms are related via a common C-terminal domain. The shared feature of RTN proteins is their association with membranes of ER (van de Velde *et al.*, 1994). Nogo-A, which is the largest of the RTN proteins, has sequences essential for inhibition of neurite growth encoded by the terminal exon (Oertle and Schwan, 2003).

The exact function of the RTNs is also unknown. Oertle and Schwab (2003) assume RTNs would be expected to exert basic functions in the cellular machinery because they are found in almost all eukaryotic cells and organisms. Additionally, they give 4 suggestions: (1) RTNs could function as

pore or transporter complexes in the ER. (2) RTNs could function in the transport of constituents from the ER to other membrane compartments such as the Golgi, endosomes, synaptic vesicles and the plasma membrane. (3) RTNs might also play a role in structural stabilization of the ER network, for example by linking the ER to the cytoskeleton via protein-protein interactions. (4) Last but not least, RTNs could have a role in cell division. The membrane topology of RTNs is of specific interest, particularly because the two very large (35 amino acid) putative transmembrane domains could both span the membrane either once or twice.

Hence, Nogo-A may be an example of a multifunctional signal molecule. Nogo isoforms possibly have some similar functions. In addition, the functions they have in common with the RTN proteins family might generally be related to ER functions (Oertle and Schwab, 2003, van de Velde *et al.*, 1994). For example, these may be roles in protein transfer through the ER (packaging and intracellular trafficking), cell division, regulation of intracellular calcium levels and apoptosis. Further investigation of the interacting partners of Nogo-A may elucidate the above hypotheses in the future.

It remains to be determined whether neurones express Nogo-A at the cell surface. So far, there is no evidence for neurons of Nogo binding to a specific receptor as it has been proven for Ods. Huber *et al.* (2002) propose that Nogo-A could also have an intracellular function in neurons possibly related -or in addition to- the neurite growth-inhibitory activity on the cell surface of Ods.

Specifically, they assume that Nogo-A could act as a cell surface signal, repulsive, attractive, or other, for other neurons, neurites, or non-neuronal cells. Different receptors or downstream pathways may mediate the specificity of action. Thus, although signal-transducing motifs on Nogo-A have not yet been found, a function of Nogo-A as a receptor for an as yet unknown ligand is well conceivable.

Based on the above, it is tempting to hypothesise that the increased activity in ventral horn neurons of 13 weeks Tg SOD1 mice is possibly associated with the increased labelling of Nogo-A in ventral horn grey and white matter Ods of the 18 weeks Tg SOD1 mice. At the clinical stage of the 18 weeks, Nogo-A immunoreactivity was reduced in ventral horn neurons. This may be explained by the fact that this stage is defined by structural and functional loss of protein leading to cell death and consequently to a considerable loss of motor neurones. Alterations in Nogo-A expression pattern in ALS were previously stated in muscle fibres in the studies of Dupuis *et al.* (2002) and Jokic *et al.* (2005). In these studies, it has been found firstly that Nogo-A protein levels were systematically increased in the muscle of exclusively ALS patients and not in any other controls, both normal and neurological. Secondly, that the heterogeneity of the expression of Nogo-A is related to the disease severity. Elevation of expression levels of Nogo-A in the Ods at this susceptible area of spinal cord in ALS indicates the inhibitory attempt of the protein in neurite regeneration and can contribute through its

antiregenerative action, to the progressive failure of neurite regeneration attempted in previous stages.

Given that the Nogo-A protein is normally detectable in lower levels in spinal cord, as it is observed in the control sample, the disease induced increase in the inhibitory isoform Nogo-A may be contributing to an altered environment counterbalancing the axonal regenerative effort and leading to the progressive failure of motor neuron axonal regeneration in ALS. It could not be suggested though that Nogo-A levels in spinal cord tissue could be used as a diagnostic marker in ALS as it has been suggested for the muscle. The reason for this is that Nogo-A is expressed also normally in the spinal cord and according to our results we did not observed a progressive increase of the protein during the different stages of the disease. Thus, it is still complicated how Nogo-A can be chronologically related to ALS and not straight forward as the pattern of Nogo-A expression in the muscle.

However, the increased immunoreactivity we observed in our results was moderate and semi-quantitatively based, using only microdensitometry. The reason of not conducting further analysis of counting the neurons with SigmaScan software was that this procedure would be time consuming, as it would require the measuring of the neuronal diameters and their further classification, before making similar calculations we did for the glial cells. Thus, it is important to mention that, in general, the main limitation of our results is the fact that they were obtained from a 20 weeks' laboratory research.

Generally, some technical considerations give some advantages to the validity of the results of this study. Firstly, the primary antibodies were specific. This was proven firstly by the negative controls and also by the fact that the staining was specific to the cells types in agreement to the literature (neurones and Ods for Nogo-A, diffuse staining for GAP-43). In addition, in quantitative analysis, the microdensitometry was technically rigorous. Last but not least, in all experiments conducted, the immunostaining conditions, the section thickness and the magnification of the photographs were constant.

Nevertheless, in order to be more certain that up-regulation of Nogo-A and GAP-43 occurs at the CNS during the clinical stages of ALS, this study should be developed methodologically. The use of immunocytochemistry enabled us to see where the protein is, but not clearly the amount of the protein absorbance in the tissue. Thus, Western Blotting conduction may demonstrate further remarkable results or merely validate (or not) these ones presented in this study. Another limitation of this study was the restricted number of sample. In the future, a possible increase of the sample could be a valuable amendment in the methodology.

Moreover, this restriction of time did not allow us to investigate other important parameters. For example, more than one anti-Nogo antibodies could be used, which would recognise different Nogo-A regions related to its inhibitory function, such as anti-amino-Nogo antibody or anti-Nogo-66 antibody, so as to observe different patterns of staining specifically related to the inhibitory function of the protein. Also, the correlation of the time course

expression of Nogo-A and GAP-43 can be investigated using quantitative methods and statistical analysis so as to investigate the relationship between growth inhibitory (Nogo-A) and growth promoting (GAP43) molecules as an important indicator of the regenerative response during ALS.

In conclusion, our results demonstrate that Nogo-A and GAP-43 are localized in the ventral spinal cord of SOD1 mice in an increased way that is consistent with its described role as a neurite growth inhibitor. Given that the discovery of Nogo has made some exciting potentials for the development of strategies aimed at promoting CNS regeneration, the detection and description of specific inhibitory components of the CNS environment like Nogo may encourage the design of methods intended to deactivate and neutralise these molecules and thereby promote regeneration by modifying the expression of proteins like GAP-43. Finally, it is likely that the most successful policy for recovering function in ALS patients will develop a combinational approach. Such an approach though may also involve management of a number of aspects, such as levels of Nogo-A and growth promoting signals.

REFERENCES

- Afifi A. K., Aleu F. P., Goodgold J., MacKay B. (1966). *Ultrastructure of atrophic muscle in amyotrophic lateral sclerosis.* Neurology. May;16(5):475-81.
- Benowitz L. I., Routtenberg A. (1987). *A membrane phosphoprotein associated with neural development, axonal regeneration, phospholipid metabolism, and synaptic plasticity.* Trends Neurosci. 10 :527–532.
- Boillee S., Vande Velde C., Cleveland D. W. (2006) *ALS: a disease of motor neurons and their nonneuronal neighbors.* Neuron. Oct 5;52(1):39-59.
- Borchelt D. R. (2006). *Amyotrophic lateral sclerosis--are microglia killing motor neurons?* N Engl J Med. Oct 12;355(15):1611-3.
- Brittis P. A., Flanagan J. G. (2001). *Nogo domains and a Nogo receptor: implications for axon regeneration.* Neuron. Apr; 30(1):11-4.
- Brown, R. H., Meininger, V., Swash, M. (2000), *Amyotrophic Lateral Sclerosis,* Martin Dunitz Ltd. ,UK.
- Bruijn L. I., Becher M. W., Lee M. K., Anderson K. L., Jenkins N. A., Copeland N. G., Sisodia S. S., Rothstein J. D., Borchelt D. R., Price D. L., Cleveland D. W. (1997). *ALS-linked SOD1 mutant G85R mediates damage to astrocytes and promotes rapidly progressive disease with SOD1-containing inclusions.* Neuron. Feb; 18(2):327-38.

- Bruijn L. I., Miller T. M., Cleveland D. W. (2004) *Unravelling the mechanisms involved in motor neuron degeneration in ALS*. Annu Rev Neurosci. 27:723-49.
- Buss A., Sellhaus B., Wolmsley A., Noth J., Schwab M. E., Brook G. A. (2005). *Expression pattern of NOGO-A protein in the human nervous system*. Acta Neuropathol (Berl). Aug;110(2):113-9.
- Chen, M. S., Huber, A. B., van der Haar, M. E., Frank, M., Schnell, L., Spillmann, A. A., Christ, F., and Schwab, M. E. (2000). Nogo-A is a myelin-associated neurite outgrowth inhibitor and an antigen for monoclonal antibody IN-1. Nature. 403, 434–439.
- Chiu A. Y., Zhai P., Dal Canto M. C., Peters T. M, Kwon YW, Prattis SM, Gurney ME. (1995). *Age-dependent penetrance of disease in a transgenic mouse model of familial amyotrophic lateral sclerosis.* Mol Cell Neurosci. Aug;6(4):349-62.
- Clark A. W., Tran P. M., Parhad I. M., Krekoski C. A., Julien J. P. (1990). Neuronal gene expression in amyotrophic lateral sclerosis.Brain Res Mol Brain Res. Jan;7(1):75-83.
- Cluskey S., Ramsden D. B. (2001). *Mechanisms of neurodegeneration in amyotrophic lateral sclerosis.* Mol Pathol. Dec; 54(6):386-92.
- Delisle M. B., Carpenter S. (1984). *Neurofibrillary axonal swellings and amyotrophic lateral sclerosis.* J Neurol Sci. Feb;63(2):241-50.
- Dupuis L., Gonzalez de Aguilar J. L., di Scala F., Rene F., de Tapia M., Pradat P.F., Lacomblez L., Seihlan D., Prinjha R., Walsh F. S.,

Meininger V., Loeffler J. P. (2002). *Nogo provides a molecular marker for diagnosis of amyotrophic lateral sclerosis.* Neurobiol Dis. Aug; 10(3):358-65.

- Dupuis L., Gonzalez de Aguilar J. L., Oudart H., de Tapia M., Barbeito L., Loeffler J. P. (2004). *Mitochondria in amyotrophic lateral sclerosis: a trigger and a target.* Neurodegener Dis.; 1(6):245-54.
- Elliott J. L. (1999). *Experimental models of amyotrophic lateral sclerosis.* Neurobiol Dis. Oct; 6(5):310-20.
- Engelhardt J. I., Appel S. H. (1990). *IgG reactivity in the spinal cord and motor cortex in amyotrophic lateral sclerosis.*Arch Neurol. Nov; 47(11):1210-6
- Fournier, A. E., GrandPre´, T., and Strittmatter, S. M. (2001). *Identification of a receptor mediating Nogo-66 inhibition of axonal regeneration.* Nature. 409, 341–346.
- Furukawa, Y., Torres, A. S., and O'Halloran, T. V. (2004). *Oxygeninduced maturation of SOD1: a key role for disulfide formation by the copper chaperone* CCS. EMBO J. 23, 2872–2881.
- Geracitano R., Paolucci E., Prisco S., Guatteo E., Zona C., Longone P., Ammassari-Teule M., Bernardi G., Berretta N., Mercuri N. B. (2003). *Altered long-term corticostriatal synaptic plasticity in transgenic mice overexpressing human CU/ZN superoxide dismutase (GLY(93)-->ALA) mutation.* Neuroscience. 118(2):399-408.
- Gorgels T. G. M. F., Campagne M. V. L., Oestreicher A. B., Gribnau A. A. M., Gispen W. H. (1989). *B-50/GAP43 is localized at the cytoplasmic*

side of the plasma membrane in developing and adult rat pyramidal tract. J Neurosci 9 :3861–3869.

- GrandPre T., Nakamura F., Vartanian T., Strittmatter S. M. (2000). *Identification of the Nogo inhibitor of axon regeneration as a Reticulon protein.* Nature. Jan 27;403(6768):439-44.
- Grandpre T., Strittmatter S. M. (2001). *Nogo: a molecular determinant of axonal growth and regeneration.* Neuroscientist. Oct;7(5):377-86.
- Gurney M. E. (1997). *The use of transgenic mouse models of amyotrophic lateral sclerosis in preclinical drug studies.* J Neurol Sci. Oct; 152 Suppl 1:S67-73.
- Gurney M. E. (1997a). *Transgenic animal models of familial amyotrophic lateral sclerosis.* J Neurol. May;244 Suppl 2:S15-20.
- Gurney M. E. (1997b) *The use of transgenic mouse models of amyotrophic lateral sclerosis in preclinical drug studies.* J Neurol Sci. Oct;152 Suppl 1:S67-73.
- Henkel J. S., Engelhardt J. I., Siklos L., Simpson E. P., Kim S. H., Pan T., Goodman J. C., Siddique T., Beers D. R., Appel S. H. (2004) *Presence of dendritic cells, MCP-1, and activated microglia/macrophages in amyotrophic lateral sclerosis spinal cord tissue.* Ann Neurol. Feb;55(2):221-35.
- Hirano, A., Donnenfeld, H., Sasaki, S., and Nakano, I. (1984a). *Fine structural observations of neurofilamentous changes in amyotrophic lateral sclerosis.* J. Neuropathol. Exp. Neurol. 43, 461–470.

- Hirano, A., Nakano, I., Kurland, L.T., Mulder, D.W., Holley, P.W., and Saccomanno, G. (1984b). *Fine structural study of neurofibrillary changes in a family with amyotrophic lateral sclerosis.* J. Neuropathol. Exp. Neurol. 43, 471–480.
- Huber A. B., Weinmann O., Brosamle C., Oertle T., Schwab M. E. (2002). *Patterns of Nogo mRNA and protein expression in the developing and adult rat and after CNS lesions.* J Neurosci. May 1;22(9):3553-67.
- Ikemoto A., Kawanami T., Llena J. F., Hirano A. (1994). *Immunocytochemical studies on synaptophysin in the anterior horn of lower motor neuron disease.* J Neuropathol Exp Neurol 53 :196–201. Ikemoto A, Hirano A., Matsumoto S., Akiguchi I., Kimura J. (1996). *Synaptophysin expression in the anterior horn of Werdnig-Hoffmann disease.* J Neurol Sci. 136 :94–100.
- Ikemoto A., Hirano A. (1996). *Comparative immunohistochemicalstudy on synaptophysin expression in the anterior horn of post-poliomyelitis and sporadic amyotrophic lateral sclerosis.* Acta Neuropathol. 92 :473–478.
- Ikemoto A., Hirano A., Akiguchi I. (1999). *Increased expression of growth-associated protein 43 on the surface of the anterior horn cells in amyotrophic lateral sclerosis.* Acta Neuropathol (Berl). Oct;98(4):367-73.
- Jokic N., Gonzalez de Aguilar J. L., Pradat P. F., Dupuis L., Echaniz-Laguna A., Muller A., Dubourg O., Seilhean D., Hauw J. J., Loeffler J. P., Meininger V. (2005). *Nogo expression in muscle correlates with amyotrophic lateral sclerosis severity.* Ann Neurol. Apr; 57(4):553-6.

- Josephson A., Widenfalk J., Widmer H. W., Olson L, Spenger C. (2001). *NOGO mRNA expression in adult and fetal human and rat nervous tissue and in weight drop injury.* Exp Neurol. Jun;169(2):319-28
- Kage M., Ikemoto A., Akiguchi I., Kimura J., Matsumoto S., Kimura H., Tooyama I. (1998). *Primary structure of GAP-43 mRNA expressed in the spinal cord of ALS patients.* Neuroreport. May 11;9(7):1403-6.
- Kawamata T., Akiyama H., Yamada T., McGeer P. L. (1992). *Immunologic reactions in amyotrophic lateral sclerosis brain and spinal cord tissue.* Am J Pathol. Mar; 140(3):691-707
- Lenaz G., Bovina C., D'Aurelio M., Fato R., Formiggini G., Genova M. L., Giuliano G., Merlo Pich M., Paolucci U., Parenti Castelli G., Ventura B. (2002). *Role of mitochondria in oxidative stress and aging.* Ann N Y Acad Sci. Apr; 959:199-213.
- Liu H., Ng C. E., Tang B. L. (2002). *Nogo-A expression in mouse central nervous system neurons.* Neurosci Lett. Aug 16;328(3):257-60.
- Mariotti R., Bentivoglio M. (2000). *Activation and response to axotomy of microglia in the facial motor nuclei of G93A superoxide dismutase transgenic mice.* Neurosci Lett. May 12; 285(2):87-90.
- Marklund N, Fulp CT, Shimizu S, Puri R, McMillan A, Strittmatter SM, McIntosh TK. (2006). *Selective temporal and regional alterations of Nogo-A and small proline-rich repeat protein 1A (SPRR1A) but not Nogo-66 receptor (NgR) occur following traumatic brain injury in the rat.* Exp Neurol. Jan; 197(1):70-83.

- Matsumoto S., Goto S., Kusaka H., Ito H., Imai T. (1994). *Synaptic pathology of spinal anterior horn cells in amyotrophic lateral sclerosis: an immunohistochemical study.* J Neurol Sci. 125 :180–185
- McComas A. J. (1991). *Invited review: motor unit estimation: methods, results, and present status.* Muscle Nerve. Jul;14(7):585-97.
- McGeer P. L., McGeer E. G., Kawamata T., Yamada T., Akiyama H. (1991). *Reactions of the immune system in chronic degenerative neurological diseases.* Can J Neurol Sci. Aug; 18(3 Suppl):376-9.
- Meiri K. F., Pfenninger K. H., Willard M. B. (1986). *Growth-associated protein, GAP43, a polypeptide that is induced when neurons extend axons, is a component of growth cones and corresponds to pp46, a major polypeptide of a subcellular fraction enriched in growth cones.* Proc Natl Acad Sci USA 83 :3537–3541.
- Morrison B. M., Janssen W. G., Gordon J. W., Morrison J. H. (1998a). *Time course of neuropathology in the spinal cord of G86R superoxide dismutase transgenic mice.* J Comp Neurol. Feb 2;391(1):64-77.
- Morrison B. M., Morrison J. H., Gordon J. W. (1998). *Superoxide dismutase and neurofilament transgenic models of amyotrophic lateral sclerosis.* J Exp Zool. Sep-Oct 1; 282(1-2):32-47.
- Oertle T., Schwab M. E. (2003). *Nogo and its paRTNers.* Trends Cell Biol. Apr;13(4):187-94.
- Oertle T., Klinger M., Stuermer C. A., Schwab M. E. (2003a). *A reticular rhapsody: phylogenic evolution and nomenclature of the RTN/Nogo gene family.* FASEB J. Jul;17(10):1238-47.

- Oertle T., van der Haar M. E., Bandtlow C. E., Robeva A., Burfeind P., Buss A., Huber A. B., Simonen M., Schnell L., Brosamle C., Kaupmann K., Vallon R., Schwab M. E. (2003b). *Nogo-A inhibits neurite outgrowth and cell spreading with three discrete regions.* J Neurosci. Jul 2;23(13):5393-406.
- Osei-Lah A. D., Turner M. R., Andersen P. M., Leigh P. N., Mills K. R. (2004). *A novel central motor conduction abnormality in D90A-homozygous patients with amyotrophic lateral sclerosis.* Muscle Nerve. Jun;29(6):790-4.
- Parhad I. M., Oishi R., Clark A. W. (1992). *GAP-43 gene expression is increased in anterior horn cells of amyotrophic lateral sclerosis.* Ann Neurol. Jun;31(6):593-7.
- Perrin F. E., Boisset G., Docquier M., Schaad O., Descombes P., Kato A. C. (2005). *No widespread induction of cell death genes occurs in pure motoneurons in an amyotrophic lateral sclerosis mouse model.* Hum Mol Genet. Nov 1; 14(21):3309-20.
- Prinjha, R., Moore, S.E., Vinson, M., Blake, S., Morrow, R., Christie, G., Michalovich, D., Simmons, D.L., and Walsh, F.S. (2000). *Inhibitor of neurite outgrowth in humans.* Nature 403, 383–384.
- Radi R., Cassina A., Hodara R. (2002). *Nitric oxide and peroxynitrite interactions with mitochondria.* Biol Chem. Mar-Apr; 383(3-4):401-9.
- Ramon y Cajal, S. (1928). *Degeneration and Regeneration of the Nervous System.* Hafner. New York.

- Ripps M. E., Huntley G. W., Hof P. R., Morrison J. H., Gordon J. W. (1995). *Transgenic mice expressing an altered murine superoxide dismutase gene provide an animal model of amyotrophic lateral sclerosis.* Proc Natl Acad Sci U S A. Jan 31;92(3):689-93.
- Rothstein J. D., Tsai G., Kuncl R. W., Clawson L., Cornblath D. R., Drachman D. B., Pestronk A., Stauch B. L., Coyle J. T. (1990). *Abnormal excitatory amino acid metabolism in amyotrophic lateral sclerosis.* Ann Neurol. Jul;28(1):18-25.
- Rowland L. P., Shneider N. A. (2001). *Amyotrophic lateral sclerosis.* N Engl J Med. May 31; 344(22):1688-700.
- Sasaki S., Maruyama S. (1994). *Synapse loss in anterior horn neurons in amyotrophic lateral sclerosis.* Acta Neuropathol. 88 :222–227.
- Schwab, M. E. and Bartholdi, D. (1996). *Degeneration and regeneration of axons in the lesioned spinal cord.* Physiol. Rev. 76, 319–370.
- Schwab J. M., Tuli S. K., Failli V. (2006). *Nogo receptor complex: confining molecules to molecular mechanisms.* Trends Mol Med. Jul;12(7):293-7.
- Skene J. H. P., Virag I. (1989) *Post-translational membrane attachment and dynamic fatty acylation of a neuronal growth cone protein, GAP43.* J Cell Biol 108 :623–62.
- Skene J. H. P., Willard M. (1981a). *Axonally transported proteins associated with axon growth in rabbit central and peripheral nervous systems.* J Cell Biol. 89 :96–103.

- Skene J. H. P., Willard. M (1981) *Electrophoretic analysis of axonally transported proteins in toad retinal ganglion cells.* J Neurochem 37 :79–87.
- Stieber A., Gonatas J. O., Collard J., Meier J., Julien J., Schweitzer P., Gonatas N. K. (2000a) *The neuronal Golgi apparatus is fragmented in transgenic mice expressing a mutant human SOD1, but not in mice expressing the human NF-H gene.* J Neurol Sci. Feb 1;173(1):63-72.
- Stieber A., Gonatas J. O., Gonatas N. K. (2000b). *Aggregation of ubiquitin and a mutant ALS-linked SOD1 protein correlate with disease progression and fragmentation of the Golgi apparatus.* J Neurol Sci. Feb 1;173(1):53-62.
- Stieber A, Gonatas JO, Gonatas NK. (2000c). *Aggregates of mutant protein appear progressively in dendrites, in periaxonal processes of oligodendrocytes, and in neuronal and astrocytic perikarya of mice expressing the SOD1(G93A) mutation of familial amyotrophic lateral sclerosis.* J Neurol Sci. Aug 15;177(2):114-23.
- Teng F. Y., Ling B. M., Tang B. L. (2004). *Inter- and intracellular interactions of Nogo: new findings and hypothesis.* J Neurochem. May;89(4):801-6.
- Teng F. Y., Tang B. L. (2005). *Nogo signaling and non-physical injury-induced nervous system pathology.* J Neurosci Res. Feb 1;79(3):273-8.
- Troost D., Claessen N., van den Oord J. J., Swaab D. F., de Jong J. M. (1993). *Neuronophagia in the motor cortex in amyotrophic lateral sclerosis.* Neuropathol Appl Neurobiol. Oct;19(5):390-7 1-707
- Turner M. R., Cagnin A., Turkheimer F. E., Miller C. C., Shaw C. E., Brooks D. J., Leigh P. N., Banati R. B. (2004). *Evidence of widespread*

cerebral microglial activation in amyotrophic lateral sclerosis: an [11C](R)-PK11195 positron emission tomography study. Neurobiol Dis. Apr;15(3):601-9

- Van de Velde H. J., Roebroek A. J., Senden N. H, Ramaekers F. C., Van de Ven W. J. (1994). *NSP-encoded reticulons, neuroendocrine proteins of a novel gene family associated with membranes of the endoplasmic reticulum.* J Cell Sci. Sep; 107 (Pt 9):2403-16.
- Wang K. C., Kim J. A., Sivasankaran R., Segal R., He Z. (2002). *P75 interacts with the Nogo receptor as a co-receptor for Nogo, MAG and OMgp.* Nature. Nov 7; 420(6911):74-8.
- Wong P. C., Pardo C. A., Borchelt D. R., Lee M. K., Copeland N. G., Jenkins N. A., Sisodia S. S., Cleveland D. W., Price D. L. (1995). *An adverse property of a familial ALS-linked SOD1 mutation causes motor neuron disease characterized by vacuolar degeneration of mitochondria.* Neuron. Jun;14(6):1105-16.
- Xu, Z., Cork, L.C., Griffin, J.W., and Cleveland, D.W. (1993). *Increased expression of neurofilament subunit NF-L produces morphological alterations that resemble the pathology of human motor neuron disease.* Cell 73, 23–33.